ISSN 1580-4003

THE SCIENTIFIC JOURNAL OF THE VETERINARY FACULTY UNIVERSITY OF LJUBLJANA

SLOVENIAN VETERINARY RESEARCH

SLOVENSKI VETERINARSKI ZBORNIK

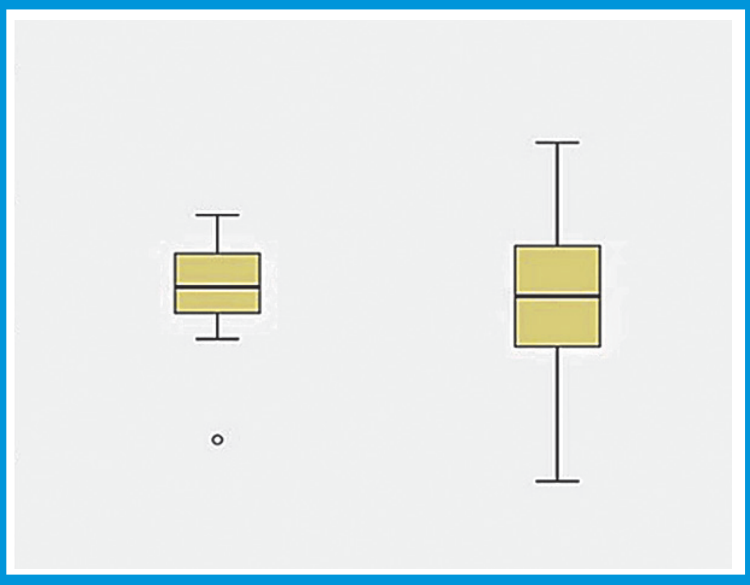

Slov Vet Res 2022; 59 (4): 169–222

Volume 59 4

Slov Vet Res • Ljubljana • 2022 • Volume 59 • Number 4 • 169–222

THE SCIENTIFIC JOURNAL OF THE VETERINARY FACULTY UNIVERSITY OF LJUBLJANA

SLOVENIAN VETERINARY RESEARCH

SLOVENSKI VETERINARSKI ZBORNIK

Volume 59 4

Slov Vet Res • Ljubljana • 2022 • Volume 59 • Number 4 • 169–222

The Scientific Journal of the Veterinary Faculty University of Ljubljana

SLOVENIAN VETERINARY RESEARCH
SLOVENSKI VETERINARSKI ZBORNIK

Previously: RESEARCH REPORTS OF THE VETERINARY FACULTY UNIVERSITY OF LJUBLJANA
Prej: ZBORNIK VETERINARSKE FAKULTETE UNIVERZA V LJUBLJANI

4 issues per year / Izhaja štirikrat letno
Volume 59, Number 4 / Letnik 59, Številka 4

Published by / Založila: University of Ljubljana Press / Založba Univerze v Ljubljani
For the Publisher / Za založbo: Gregor Majdič, the Rector of the University of Ljubljana / rektor Univerze v Ljubljani

Issued by / Izdala: Veterinary Faculty University of Ljubljana / Veterinarska fakulteta Univerze v Ljubljani
For the Issuer / Za izdajatelja: Breda Jakovac Strajn, the Dean of the Veterinary Faculty / dekanja Veterinarske fakultete

Address: Veterinary Faculty, Gerbičeva 60, 1000 Ljubljana, Slovenia
Naslov: Veterinarska fakulteta, Gerbičeva 60, 1000 Ljubljana, Slovenija
Tel.: +386 (0)1 47 79 100, Fax: +386 (0)1 28 32 243
E-mail: slovetres@vf.uni-lj.si

Sponsored by the Slovenian Research Agency
Sofinancira: Javna agencija za raziskovalno dejavnost Republike Slovenije

ISSN 1580-4003
Printed by/tisk: DZS, d.d., Ljubljana, December 2022
Number of copies printed / Naklada: 220
Indexed in/indeksirano v: Agris, Biomedicina Slovenica, CAB Abstracts, IVSI
Urlich's International Periodicals Directory, Science Citation Index Expanded,
Journal Citation Reports – Science Edition
https://www.slovetres.si/

SLOVENIAN VETERINARY RESEARCH
SLOVENSKI VETERINARSKI ZBORNIK

Slov Vet Res 2022; 59 (4)

Review Article

Rajčević U, Smole A. Preclinical mouse models in adoptive cell therapies of cancer 173

Original Research Articles

Parlak K, Naseri A, Yalcin M, Akyol E T, Ok M, Arican M. Evaluation of trauma scoring and endothelial glycocalyx injury in cats with head trauma 185

El-Bahr SM, Al-Sultan S, Hamouda AF, Atwa SAE, Abo-Kora SY, Amin AA, Shousha S, Alhojaily S, Alnehas A, Elzogby RR. Pectin improves hemato-biochemical parameter, histopathology, oxidative stress biomarkers, cytokines and expression of hepcidin gene in lead induced toxicity in rats 195

Case Report

Wu B, Wang J, Cai T, Wang C, Li D, Deng L, Peng X. Pathological findings in an old female giant panda – a case report 211

Author Index Volume 59, 2022 219

Slov Vet Res 2022; 59 (4): 173–84
DOI 10.26873/SVR-1513-2022
UDC 606:616-056.7:616-006.4:602.68:606:61:615.37:57.084

Review Article

PRECLINICAL MOUSE MODELS IN ADOPTIVE CELL THERAPIES OF CANCER

Uroš Rajčević[1]*, Anže Smole[2]*

[1]Lek, d.d., Technical Research and Development, Kolodvorska cesta 27, 1234 Mengeš, Slovenia, [2]National Institute of Biology, Department of Genetic Toxicology and Cancer Biology, Immunology and Cellular Immunotherapy (ICI) Group, 1000 Ljubljana, Slovenia

*Corresponding author, E-mail: uros.rajcevic@novartis.com, anze.smole@nib.si

Abstract: Engineered T cell-based therapies are an advanced approach for cancer immunotherapy using genetically modified T cells. To date, CD19 and BCMA targeting Chimeric Antigen Receptor (CAR) T cells have been approved for the treatment of certain hematologic malignancies. The success of CAR-T cells is offset by limited efficacy, particularly in solid tumors, and safety risks. Preclinical *in vivo* research, which is highly dependent on reliable mouse models, has been a cornerstone of the success story of adoptive cell therapies and continues to provide invaluable information for the development of the next generation of cellular immunotherapies. In this review we describe four of the most common preclinical mouse models: xenograft models, syngeneic models, immunocompetent transgenic models and humanized mouse models. All of these have advantages and disadvantages and no mouse model can fully recapitulate the human situation because of inherent differences and treatment complexity. Reports suggest that using a combination of mouse models in preclinical *in vivo* research prior to translating the treatment to humans in clinical trials can help incrementally improve the quality, safety, and efficacy of the treatment and provide more comprehensive information than a single model.

Key words: mouse model; xenograft; syngeneic; transgenic; humanized; CAR-T; adoptive cell therapy

Introduction

Adoptive cell therapy (ACT) is a next-generation approach to treating cancer based on immune cells engineered to specifically recognize and effectively eliminate cancer cells. T-cell therapy using chimeric antigen receptors (CARs) has emerged as a leading approach in ACT (1). CARs are designed receptor molecules that merge specificity of monoclonal antibodies with the signalling capacity and effector functions of the T cell receptor (TCR) in T cells (2). The initial CAR designs, referred to as first-generation CARs, include an extracellular antigen-binding domain, usually in the form of a single-chain variable fragment (scFv) derived from an antibody, linked to intracellular signalling domains, most often derived from the components of the TCR complex, such as the CD3 zeta chain (3, 4). This molecule is capable of recognizing antigens independently of HLA (human leukocyte antigens) presentation but does not support long-term T cell persistence and effector responses due to its limited signalling capacity (5). The second-generation CAR design incorporates additional co-stimulatory domains such as CD28 and 4-1BB (TNFRSF9) that enhance expansion, effector functions and persistence of CAR-T cells (2). The second-generation CAR-T design was the basis for successful clinical trials in relapsed or refractory paediatric and adult blood malignancies (6-10) that have led the U.S. Food and Drug Administration (FDA) and the European Medicines Agency (EMA) to approve CD19-targeting CAR-T cells in 2017

Received: 29 June 2022
Accepted for publication: 16 September 2022

and 2018, respectively and BCMA-targeting CAR-T cells in 2021 (11). However, adoptive cancer immunotherapy is associated with safety risks such as cytokine release syndrome (CRS) and neurologic toxicities (12), which have led to life-threatening complications (13). In addition, the efficacy of cellular immunotherapy in solid tumor as well as hematologic malignancies is limited, due in part to the immunosuppressive tumor microenvironments, intrinsic T-cell dysfunction (14) and lack of unique surface antigens (15). Various approaches have been pursued to increase the efficacy of adoptive immunotherapy in cancer, and preclinical mouse models are currently irreplaceable to validate their efficacy and safety. Excellent reviews present the use of preclinical models for adoptive cell therapies (16-18). Here, we focus on how preclinical mouse models have supported recent advances in the development of next-generation cellular immunotherapies.

Human xenograft models

A xenograft is a cell, tissue, or organ transplant from a donor that is of a different species then the recipient. In the use of mouse models for the study of human diseases, the most common type of xenograft is the transfer of human tissue, including cells and biopsies, to a mouse recipient. The recipient must be immunocompromised to avoid rejecting foreign human cells. Cells are applied either non-original place (ectopic model) or in the organ from which the tissue is derived (orthotopic model) (reviewed in (19)). In this way, researchers can translate *in vitro* findings into preclinical *in vivo* stage to evaluate the efficacy and safety of cellular immunotherapy in a given disease.

Patient-derived cancer xenografts (PDX) are a simulation of a specific patient's tumor in an animal model. The various types of immunocompromised mice used in tumor xenograft models lack part or most of the immune system so they cannot reflect the immune system of humans. Their immune response to tumors is simplified and does not capture the full complexity of the response. In the past, different types of immunocompromised mice were developed to mimic the human immune system to varying degrees.

The development of immunocompromised mice dates back to athymic mice reported as early as 1966 (20), non-obese diabetic severe combined immune-deficient mice (NOD SCID) and improved NOD SCID mice with Interleukin 2 Receptor Subunit Gamma (IL2Rg) deficiency (16, 21, 22). Since then, the use of NSG (NOD SCID IL2Rg-) (reviewed in (23)) in CAR-T has been reported by several authors including (24). The NSG mouse was developed by backcrossing the *Il2rg−/−*mouse resulting from a complete null mutation onto NOD/ShiLtSz-Prkdc SCID mouse (25). The NOG mouse was developed by backcrossing the *Il2rg−/−* mouse resultin from a truncated intracellular signaling domain onto NOD/ShiLtSz-Prkdc SCID mouse (26). In NOG mice, the *Il2rg* mutant gene is expressed and produces a protein that binds cytokines but does not signal. Conversely, *Il2rg* gene expression does not occur in NSG mice (27, 28). The use of the xenograft models gives us opportunity to assess the effect of the human CAR-T cells on human tumors but there are no interactions with other immune cells or healthy tissues. Nevertheless, xenograft models are often used as the initial preclinical mouse model in proof-of-concept studies in the development of next-generation cellular immunotherapies. They also allow functional validation of engineered human T cells including tumor targeting, anti-tumor activity, secretion of cytokines, tonic signaling, and intrinsic dysfunction such as T cell exhaustion. Here are selected recent examples that represent only a snapshot of numerous studies in this highly active and explored field of research.

As described in the introduction, the development of second-generation CAR-T cells that contain costimulatory domains in addition to CD3 zeta has been critical for clinical efficacy. Currently, so-called third-generation CAR-T cells, which integrate multiple costimulatory domains into the same CAR molecule, are being tested for efficacy and safety (29). Xenograft models have been useful in the development of second and third generation CAR-T cells (30). Route of administration is important in solid tumors (31). Xenograft models revealed the main differences between the two domains, CD28 and 4-1BB (TNFRSF9). Exhaustion was ameliorated by 4-1BB (TNFRSF9) and exacerbated by CD28 (32). CD28 promoted faster tumor regression, while 4-1BB (TNFRSF9) promoted multiple cytokine secretion (33).

CAR-T cells, which can be remotely controlled by the addition of small-molecule were tested

in immunodeficient NSG mice. The authors demonstrated that the use of a split receptor, in which antigen recognition and intracellular signaling domains assemble into a functional unit only after the addition of a heterodimerizing small molecule, allows remote control of the activity of the engineered CAR-T cells. Such regulation provides additional control of the T cell activity, with the rationale of improving safety (34).

Another landmark study at the interface between cellular immunotherapy and synthetic biology is the development of designer T cells equipped with tailored therapeutic response programs through the use of synthetic Notch receptors (synNotch). Using NSG mice with subcutaneously implanted CD19 negative or CD19 positive target cells, authors demonstrate that their system functions as designed *in vivo*. Specifically, they demonstrated *in vivo* expression of cytokines and bi-specific tumor-targeting antibodies by the SynNotch T Cells (35).

Distinct approach that allows additional control over the injected CAR-T cells to increase safety, but also to allow multiple antigen targeting to mitigate potential antigen escape in CAR-T cell therapy, is the prototype universal immune receptor called SpyCatcher. This universal immune receptor enables covalent binding of targeting ligands to the T cell surface using SpyCatcher-SpyTag chemistry. The SpyCatcher immune receptor redirects primary human T cells by addition of SpyTag-labeled targeting ligands *in vivo* in a solid tumor xenograft model. (36).

As mentioned in the introduction, intrinsic dysfunction of T cells is one of the important limiting factors in cellular immunotherapies. One such example is T cell exhaustion, which leads to defects in T cell functionalities. In an attempt to counteract exhaustion, CAR-T cells were engineered to overexpress the transcription factor c-Jun. In this study, human xenograft models in immunocompromised NOD-SCID-*Il2rg*−/− (NSG) mice were used as models to demonstrate enhanced expansion, improved function, limited terminal differentiation and enhanced anti-tumor activity (37).

Current clinically used CAR-T cells use lentiviral or retroviral vectors to introduce CARs into primary T cells. While this is effective, it poses certain problems related to random integration. With the advent of genome editing approaches most notably CRISPR/Cas systems, the CARs (38) or TCRs (39, 40) were introduced into the endogenous TCR genomic locus. These protocols utilize CRISPR/Cas9 and the homology-directed repair (HDR) pathway with either viral (38) or non-viral (39, 40. 41) donor template delivery. Both landmark approaches were validated in NOD/SCID/ IL2gr-null (NSG) xenograft models. In these studies, xenograft models were sufficient to provide evidence of the concept of these novel platforms, specific targeting and tumor control, as well as improved functionalities of human T cells engineered with designed immune receptors.

Tasian reports that CAR-T's orchestration of off-target toxicities may only be found in early clinical trials (41). Mouse xenografts are useful in screening for basic CAR-T efficacy and for answering specific human biology questions. Additional studies in immune competent hosts are required to evaluate CAR safety. The hostile tumor microenvironment (TME) includes Tregs and MDSCs, but it's largely ignored in preclinical immunocompromised models (42). Tregs may partially explain worse CAR-T clinical trial results in solid tumors, and their inclusion in xenograft models may provide more accurate results.

In xenograft models it is difficult to distinguish between xenogeneic rejection, graft versus host disease (GVHD), allogenic response of human CAR-T cells to the tumor and actual CAR-T therapeutic efficacy. Therefore, appropriate and rigorous controls in experimental design are very important to obtain reliable results and draw correct conclusions. One such control that aids in differentiating the above-mentioned effects from the on-target responses of designed cellular immunotherapies are T cells engineered with a non-targeting immune receptor, such as CAR directed against target that is not expressed on tumor cells. In the absence of the host immune system, it is not possible to test the TME, tumor metastatic potential, or host response to CAR-T.

Taken together, xenograft models provide key insights into the function of human CAR-T cells against human tumors *in vivo*, which has been a basis for clinical success. This allowed the study of basic properties of human CAR-T cells such as anti-tumor activity, secretion of cytokines, expansion and persistence *in vivo*. However, in the absence of an interacting immune system, these models do not allow for comprehensive evaluation of immune-mediated mechanisms as well as on-target off-tumor toxicities (Figure 1).

To gain deeper insight into mechanism of action, interactions with the endogenous immune system and the role of endogenous immune response, xenograft models need to be complemented with syngeneic mouse models.

Syngeneic mouse models

Syngeneic models refer to genetically identical or sufficiently identical and immunologically compatible individuals to allow transplantation. The main feature of syngeneic mouse models is their immunocompetence, including full mouse immunity and comprehensive stroma. Important factor in their comprehensive use is their relative simplicity compared with other immunocompetent models.

The field of engineered cellular immunotherapies is moving towards increasing the efficacy and improving safety. Often, designed T cells rely upon recruiting endogenous immune response or counteracting immunosuppressive TME. Elucidation of the effects and mechanisms cannot be performed in a comprehensive manner in immunocompromised mice because the interacting immune system is lacking. Here, we list selected reports of upgraded CAR-T cells whose functions have been studied in various syngeneic mouse models.

In preclinical studies of adoptive cell therapy in a syngeneic model, the CAR-T, tumors, and target antigens are all mouse derived. Thus, the model allows observation of the CAR-T cells in the context of a functional immune system (16). This model can reveal-on-target off-tumor toxicity (43). Its major drawback is that mouse biology does not fully recapitulate human biology. Mouse syngeneic models have largely been unable to mimic CRS. Mouse CAR-T have shorter persistence and are more susceptible to activation–induced cell death compared to human. Syngeneic models do not provide much insight into the mechanisms of human CAR-T cells (44).

Initial syngeneic models of CAR-T demonstrated the superior efficiency of CAR-T over monoclonal antibodies. Preconditioning of the patient by irradiation or chemoablation was crucial for the efficacy of CAR-T therapy (45, 46). In this way, B-cell aplasia was shown as toxicity – mice were clear of lymphoma, but B cells were also absent. Cheadle (47) showed that first generation CAR-T were efficient in removing lymphoma, but not persistent. Second generation CAR-T cells induced B-cell aplasia and chronic toxicity accompanied by CD11b+Gr1+ myeloid derived suppressor cells; elevated TNFα and IFNγ point toward CRS–BALB/c (48), but not in C3H/HeJ or C57BL/6J – side effects vary between strains.

Better and more accurate preclinical models are needed for CAR-T in solid tumors. There the combination with checkpoint blockade regimens was shown to be successful (49). Syngeneic model also demonstrated potential toxicities and strain-specific effects (50). Chinnasamy (51) emphasized that mouse strains must be carefully selected or tested on multiple strains to ensure that toxicity is accurately modeled.

Widely varying results in studies using the same tumor associated antigen (TAA) but different mouse strains as seen in anti-CD19, anti-NKG2D and anti-VEGF studies caution against using a single mouse strain to determine safety before moving to clinical trials (16).

One approach to generate CAR-T cells with improved functionalities is to overexpress an additional accessory molecule along with the immune receptor. Constitutive expression of IL-12 in CAR-T cells was shown to augment CAR-T cell functions in a syngeneic model. Additional modification of infused hCD19-targeted CAR-T cells to secrete IL-12 allowed for efficient eradication of systemic EL4 (hCD19) tumors, as well as induction of B-cell aplasias, in the absence of prior cyclophosphamide conditioning. This outcome was dependent on both CD4 and CD8 T-cell subsets and required continued *in vivo* autocrine stimulation of IL-12 as well as modified T cell–IFNγ secretion, which in turn resulted in resistance to Treg-mediated suppression (52).

In addition to IL-12, IL-18 emerged as a promising candidate (53-56). In one of these studies (54) syngeneic model of pancreatic and lung tumors revealed that release of IL-18 modulated the immune cell landscape in the tumor. Increased numbers of CD206- M1 macrophages and NKG2D+ NK cells were observed, while Tregs, suppressive $CD103^{+}$ DCs, and M2 macrophages decreased. These observations were possible because an intact interaction immune system was present.

CAR-T cells were also engineered to secrete a combination of IL-7+CCL19 with the rationale that these factors contribute to the maintenance of T-cell zones in lymphoid organs. Upgraded CAR-T cells eradicated established solid tumors

and prolonged survival compared to conventional CAR-T cells. The syngeneic model showed increased infiltration of dendritic cells and T cells into tumor tissues. Depletion of recipient T cells reduced the therapeutic effects of upgraded CAR-T cell treatment, demonstrating that endogenous immune responses were induced (57).

In another study, CAR-T cells were engineered to secrete single-chain variable fragments (scFv) that block PD-1 (PDCD1). Clinically relevant syngeneic model with PD-L1 (CD274) positive tumor targets made it possible to demonstrate that secreted scFv acted on both CAR-T cells and bystander tumor-specific T cells to improve anti-tumor activity (58).

CAR-T cells constitutively expressing the immune-stimulatory molecule CD40 ligand (CD40L) demonstrated improved anti-tumor activity. In relevant syngeneic models, the authors investigated the underlying mechanisms and found that CD40L+ CAR-T cells were able to counteract tumor antigen escape variants via CD40/CD40L-mediated cytotoxicity and induction of an endogenous immune response. After adoptive cell transfer, upgraded CAR-T cells licensed antigen-presenting cells and recruited endogenous tumor-recognizing T cells (59).

Another study demonstrating the importance of syngeneic mouse models explored how depletion of immunosuppressive M2 tumor-associated macrophages (TAMs) may improve the efficacy of CAR-T cells. The authors found that a folate receptor β (FRβ) positive subset of TAMs exhibited an immunosuppressive M2-like profile. When CAR-T cells were engineered to eliminate these FRβ+ TAMs, an enrichment of proinflammatory monocytes, a recruitment of endogenous tumor-specific CD8+ T cells, delayed tumor growth, and prolonged survival were observed (60).

Syngeneic models are useful for evaluating immunotherapies, *e.g.* in combination studies, particularly using checkpoint inhibitors. Syngeneic model panels can be extensively characterized (e.g. RNA sequencing of cell lines and tumors, immunophenotyping, biomarker identification), and these data can be combined with *in vivo* efficacy benchmarking profiling results from common checkpoint inhibitors (anti-PD-1, PD-L1, CTLA-4).

Syngeneic models are therefore an indispensable for evaluating the safety and efficacy of cellular immunotherapy, as they allow the study of adoptively transferred cells in the context of an interacting immune system. This allows for a rigorous assessment of immune-mediated mechanisms involved in successful therapy as well as toxicities. Potential drawbacks of syngeneic models include difficulties in generating cellular products and limited persistence and efficacy after infusion (Figure 1).

Immunocompetent transgenic mice

Transgenic animals have been around for several decades (61). Immunocompetent transgenic mice tolerant to human tumor associated antigens (TAAs) have been described in hematologic and solid tumors and for evaluating the safety and efficacy of antitumor immunotherapies (62-67). Although most anti CD19 CAR-Ts are studied in syngeneic or xenograft models, immunocompetent transgenic mouse models can also be used to better determine CAR-T safety. In transgenic mice, human TAA (murine TAA knockout and human TAA knock in) are expressed in mice to highlight the on-target off-tumor effect in healthy tissues. The mice are bred to have TAA expression similar to humans (68). Mice have their own T cells and an intact immune system (like in syngeneic models), but allow the use of human TAA-specific CAR-Ts (like xenografts) (16). A study in C57BL/6J with mouse CD19 knockout and human CD19 knockng restricted to B cells showed no toxicities other than B-cell aplasia (52). CARs targeting different antigens (CD19, CEA, HER2) have been tested in the clinic. The positive effect of preconditioning on adoptively transferred cells was confirmed in transgenic and not xenograft models (16, 69, 70). Engrafted tumors do not recapitulate many of the properties of naturally occurring tumors. A transgenic model in which tumors develop spontaneously can better mimic clinical progression and predict off-tumor toxicities (16). Transgenic CEA mice were developed by Zimmerman and colleagues (71) and have been frequently used to test CEA-targeting- CAR-T-cell therapy. In this model with high CEA expression, the toxicity associated with CAR-T cells appears to be limited to high-affinity CAR-T cells (65, 67). One of transgenic mouse models with CEA levels equivalent to those in humans (72) has also shown severe side effects associated with CAR-T-cell therapy (73, 74).

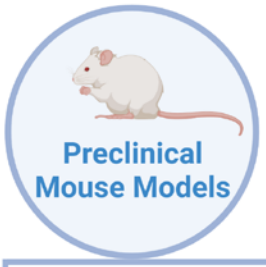

	Cancer cells	CAR-T cells	Interacting Immune/Host Environment	Pros	Cons
Human Xenograft	Human	Human	Immunodeficient Mouse	•Human CAR-T vs human cancer cells •Evaluation of fundamental CAR-T cells properties	•Interacting immune system is lacking •No ON-target OFF-tumor toxicity evaluation •GVHD
Syngeneic	Mouse	Mouse	Immunocompetent Mouse	•Interacting immune system is present •Evaluation of immune mediated mechanisms	•Tumor engraftment can be challanging •Preconditioning may be required •Limited persistance of transfered CAR-T cells
Transgenic	Mouse	Mouse	Immunocompetent Mouse	•Interacting immune system and expression of target antigens on host tissues enables the studies of ON-target OFF-tumor effects	•Expression of target antigens may not correlate between human and mouse •Limited recapitulation of spontaneous tumors
Humanized	Human	Human	Human (HSPCs)	•Human CAR-T cells vs human cancer cells in the presence of the engrafted human immune cells •CRS and neurotoxicity evaluation	•Difficult and complex model •Requirement of HSPCs engraftment

Figure 1: Schematic representation of preclinical mouse models for adoptive cell therapies

Figure created with BioRender.com

Humanized models

Currently, NOD/SCID/*Il2rg*−/− (NSG) or BALB/c/RAG2−/−/*Il2rg*−/− (BRG) mice are the standard recipients in the generation of humanized mice because they are deficient in mouse T cells, B cells, and NK cells (75-77). Transfer of human CD34+ hematopoietic stem and progenitor cells (HSPCs) into newborn NSG or BRG mice results in long-term engraftment of CD34+ cells and reconstitution of multilineage human immune cells (77-79). The comprehensive transfer protocol involves transfer of human CD34+ cells into NSG recipient mice and implantation of human fetal thymus and liver tissue under the kidney capsule of these mice (77, 80, 81). The resulting humanized mice are called bone marrow-liver-thymus (BLT) mice. They support the long-term engraftment and systemic reconstitution of a nearly complete human immune system, including multilineage human adaptive and innate immune cells consisting of T cells, B cells, NK cells, dendritic cells, and macrophages (77, 80, 81). Importantly, human immune cells developed in BLT mice, particularly T cells, are functional and have shown productive responses to skin xenografts and various viral/bacterial infections (77, 80-82). The next generation of humanized mouse models including NSG-SGM3 (or NSGS), NSGW41, NOG-EXL and MISTRG, support human myelopoiesis at varying degrees and through different strategies (28).

Humanized mouse models may bridge the gap between the syngeneic and xenograft models, because they are tolerant to human cells and exhibit aspects of a functional human immune system (16).

Until recently, CRS, which typically develops within the first few days after infusion of CD19 CAR-T cells, and neurotoxicity, the two major toxicities associated with clinically used CD19 CAR-T cells in humans, could not be reproduced in preclinical mouse models. This changed with

the development of a novel xenograft model in humanized mice that faithfully recapitulated both major toxicities (83). This model was developed by engrafting human cord blood hematopoietic stem and progenitor cells (HSPCs) into sub lethally irradiated newborn triple transgenic NSG (SGM3) mice. These mice express human stem cell factor, granulocyte-macrophage colony-stimulating factor (CSF2), and IL-3 to support the engraftment. Successful reconstitution of hematopoiesis was demonstrated, which included human B cells, monocytes, and T cells as well as cells from other lineages. Interestingly, the timing of HSC injection shortly after birth was important for successful human T lymphopoiesis. Circulating T cells exhibited a physiological CD4/CD8 ratio and differentiated into all major T cell differentiation subsets. T cells from these mice were then used to generate second-generation CAR-T cells targeting either CD19 or CD44v6. These CAR-T cells were injected into adult SGM3 mice that had previously been engrafted with ALL-CM leukemia cells. CAR-T cells cleared leukemia, which was associated with CRS characterized by weight loss, fever, and elevated systemic levels of human inflammatory cytokines including IL-6, resembling CRS in humans receiving CD19-targeting CAR-T cells. The authors used this model to show that monocytes are the major sources of IL-1 and IL-6 during CRS and that the syndrome could be prevented by depleting monocytes or by blocking the IL-6 receptor with tocilizumab (IL-6 receptor-blocking antibody). This model also recapitulated the lethal neurotoxicity, characterized by inflammation of the meninges. Interestingly, authors demonstrated that anakinra (IL-1 receptor antagonist) but not tocilizumab ameliorated neurotoxicity.

In the follow-up study by the same group, this model was further developed to investigate the efficacy and safety of CAR-T cells derived from preselected T cell subsets. When preselected naive/stem memory T cells were used to generate the CAR-T cellular product, superior anti-tumor activity, expansion and functional phenotype were observed compared to unselected bulk T cells. Surprisingly, this was accompanied by limited incidence of severe CRS and neurotoxicity. Overall, this model reveled improved efficacy and safety when preselected T cells are used to generate CAR-T cell products (84).

Therefore, in contrast to all other *in vivo* models using mice, humanized mouse models were able to reveal and investigate critical toxicities associated with CAR-T cell therapy (Figure 1).

In addition to humanized mouse models for T cell-based therapies, models have also been developed that allow adoptive transfer of engineered B cells. In this example, B cells were first isolated from the spleens of humanized donor mice, then genetically engineered and infused into "autologous" humanized recipient mice. Because the recipient mice were humanized with the same source of CD34+ cells as the humanized donor mice, such approach rendered enigneered human B cells tolerant to the host (85).

Conclusions

Cellular immunotherapy with CAR-T cells is a paradigm shifting approach for the treatment of certain blood cancers. However, limited efficacy and safety risks are the major barriers to advance the field and plethora of academic research groups, biotech and pharmaceutical companies are developing innovative next-generation cellular immunotherapies. After a novel approach has been validated *in vitro*, the next steps are experiments in preclinical mouse models. Typically, the initial experiments are conducted in human xenograft models, which are well suited for evaluating of novel genetic constructs and designs, immune receptor signaling, anti-tumor activity and intrinsic properties of human CAR-T cells, such as expansion and persistence, as well as certain dysfunctions, including T cell exhaustion. When more in-depth information about the immune mechanisms is required, which is the case when improved cellular immunotherapies aim to recruit endogenous immune responses and/or counteract an immunosuppressive tumor microenvironment, xenograft models are inadequate because they lack an interacting immune response. To answer such questions, syngeneic models are needed and have already provided valuable information for clinical translation. Since syngeneic models are associated with certain challenges including difficulties in the manufacturing of mouse cellular products, *in vivo* expansion, persistence, and efficacy, studies that systematically develop optimized protocols and procedures are very important (86).

In human clinical trials using CAR-T cells, certain toxicities including CRS and neurotoxicity

were observed that were not predicted by any of the preclinical models available at the time. Recently, a humanized mouse model was successfully developed to specifically address this challenge and replicate the pathologies observed in humans in preclinical mouse models as well (83). This example highlights the importance of continued development of preclinical mouse models as the field of cellular immunotherapy rapidly grows.

Preclinical mouse models continue to be a cornerstone in the development of the next generation of cellular immunotherapies. In this review recent advances and use of the four most common preclinical mouse models are presented. In addition, we presented the selected recent studies in which these models have been used to demonstrate innovative CAR-T cell approaches. The use of multiple models may provide a better understanding of a particular CAR-T therapy than a single model and we anticipate that increasingly sophisticated models will be developed, aided in part by recent advances in genome editing technologies, to comprehensively address the complexities of immunology and cellular immunotherapy. However, we must be aware of the limitations of preclinical mouse models, including the inherent differences between human and mouse biology and immunology. Careful design of properly controlled experiments is essential to generate reliable, high-quality data and draw the right conclusions required for clinical translation of cellular immunotherapies.

Acknowledgements

We thank K. Butina Ogorelec for reviewing and providing valuable feedback on the manuscript. A.S. received funding from the Slovenian Research Agency (ARRS) for Project J3-3084 and Program P1-0245, and from Research fund of the National institute of biology for Project 10ICIGEN (ICI). Figures created with BioRender.com

References

1. June CH, Sadelain M. Chimeric antigen receptor therapy. N Engl J Med 2018; 379: 64–73.

2. Sadelain M, Brentjens R, Rivière I. The promise and potential pitfalls of chimeric antigen receptors. Curr Opin Immunol 2009; 21: 215–23.

3. Kuwana Y, Asakura Y, Utsunomiya N, et al. Expression of chimeric receptor composed of immunoglobulin-derived V regions and T-cell receptor-derived C regions. Biochem Biophys Res Commun 1987; 149: 960–8.

4. Eshhar Z, Waks T, Gross G, Schindler DG. Specific activation and targeting of cytotoxic lymphocytes through chimeric single chains consisting of antibody-binding domains and the gamma or zeta subunits of the immunoglobulin and T-cell receptors. Proc Natl Acad Sci U S A 1993; 90: 720–4.

5. Brocker T, Karjalainen K. Signals through T cell receptor-zeta chain alone are insufficient to prime resting T lymphocytes. J Exp Med 1995; 181: 1653–9.

6. Grupp SA, Kalos M, Barrett D, Aplenc R et al. Chimeric antigen receptor-modified T cells for acute lymphoid leukemia. N Engl J Med 2013; 368: 1509–18.

7. Maude SL, Laetsch TW, Buechner J, et al. Tisagenlecleucel in children and young adults with B-cell lymphoblastic leukemia. N Engl J Med 2018; 378: 439–48.

8. Lee DW, Kochenderfer JN, Stetler-Stevenson M, et al. T cells expressing CD19 chimeric antigen receptors for acute lymphoblastic leukaemia in children and young adults: a phase 1 dose-escalation trial. Lancet 2015; 385: 517–28.

9. Schuster SJ, Svoboda J, Chong EA, et al. Chimeric antigen receptor T cells in refractory B-cell lymphomas. N Engl J Med 2017; 377: 2545–54.

10. Sommermeyer D, Hudecek M, Kosasih PL, et al. Chimeric antigen receptor-modified T cells derived from defined CD8+ and CD4+ subsets confer superior antitumor reactivity i*n vivo*. Leukemia 2016; 30: 492–500.

11. Mullard A. FDA approves first BCMA-targeted CAR-T cell therapy. Nat Rev Drug Discov. 2021; 332: 20–5.

12. Brudno JN, Kochenderfer JN. Recent advances in CAR T-cell toxicity: mechanisms, manifestations and management. Blood Rev 2019; 34: 45–55.

13. Neelapu SS, Tummala S, Kebriaei P, et al. Chimeric antigen receptor T-cell therapy - assessment and management of toxicities. Nat Rev Clin Oncol 2018; 15: 47–62.

14. Fraietta JA, Lacey SF, Orlando EJ, et al. Determinants of response and resistance to CD19 chimeric antigen receptor (CAR) T cell

therapy of chronic lymphocytic leukemia. Nat Med 2018; 24: 563–71.

15. Johnson LA, June CH. Driving gene-engineered T cell immunotherapy of cancer. Cell Res 2017; 27: 38–58.

16. Siegler EL, Wang P. Preclinical models in chimeric antigen receptor–engineered T-cell therapy. Human Gene Ther 2017; 29: 534–46.

17. Kaushik G, Venkatesha S, Verma B, et al. Preclinical in vitro and *in vivo* models for adoptive cell therapy of cancer. Cancer J 2022; 28: 257–62.

18. Magee MS, Snook AE. Challenges to chimeric antigen receptor (CAR)-T cell therapy for cancer. Discov Med 2014; 18: 265–71.

19. Rajcevic U. A rodent brain orthotopic model to study human malignant glioma. Slov Vet Res 2011; 48: 5–14.

20. Flanagan SP. 'Nude', a new hairless gene with pleiotropic effects in the mouse. Genet Res 1966; 8: 295–309.

21. Goldman JP, Blundell MP, Lopes L, et al. Enhanced human cell engraftment in mice deficient in RAG2 and the common cytokine receptor gamma chain. Br J Haematol 1998; 103: 335–42.

22. Tyagi RK, Jacobse J, Li J, Allaman MM, et al. HLA-restriction of human treg cells is not required for therapeutic efficacy of low-dose IL-2 in humanized Mice. Front Immunol 2021; 24: e630204. doi: 10.3389/fimmu.2021.630204

23. Rodriguez-Garcia A, Watanabe K, Guedan S. Analysis of antitumor effects of CAR-T cells in mice with solid tumors. Methods Mol Biol 2020; 2086: 251–71.

24. Walsh NC, Kenney LL, Jangalwe S, et al. Humanized mouse models of clinical disease. Annu Rev Pathol 2017; 24: 187–215.

25. Shultz LD, Lyons BL, Burzenski LM, Shultz LD. Human lymphoid and myeloid cell development in NOD/LtSz-scid IL2R gamma null mice engrafted with mobilized human hemopoietic stem cells. J Immunol 2005; 174: 6477–89.

26. Ito M, Hiramatsu H, Kobayashi K, et al. NOD/SCID/gamma(c)(null) mouse: an excellent recipient mouse model for engraftment of human cells. Blood 2002 100: 3175–82.

27. Covassin L, Jangalwe S, Jouvet N, et al. Human immune system development and survival of non-obese diabetic (NOD)-scid IL2rγnull (NSG) mice engrafted with human thymus and autologous haematopoietic stem cells. Clin Exp Immunol 2013; 174: 372–88.

28. Arranz L. The hematology of tomorrow is here-preclinical models are not: cell therapy for hematological malignancies. Cancers (Basel) 2022; 14(3): e580. doi: 10.3390/cancers14030580.

29. Ramos CA, Rouce R, Robertson CS, et al. *In vivo* fate and activity of second- versus third-generation CD19-specific CAR-T cells in B cell non-Hodgkin's lymphomas. Mol Ther 2018; 26: 2727–37.

30. Maher J, Brentjens RJ, Gunset G, et al. Human T-lymphocyte cytotoxicity and proliferation directed by a single chimeric TCRzeta / CD28 receptor. Nat Biotechnol 2002; 20: 70–5.

31. Kakarla S, Chow KKH, Mata M., et al. Antitumor effects of chimeric receptor engineered human T cells directed to tumor stroma. Mol Ther 2013; 21: 1611–20.

32. Long AH, Haso WM, Shern JF, et al. 4-1BB costimulation ameliorates T cell exhaustion induced by tonic signaling of chimeric antigen receptors. Nat Med 2015; 21: 581–90.

33. Carpenito C, Milone MC, Hassan R, et al. Control of large, established tumor xenografts with genetically retargeted human T cells containing CD28 and CD137 domains. Proc Natl Acad Sci U S A 2009; 106: 3360–5.

34. Wu CY, Roybal KT, Puchner EM, et al. Remote control of therapeutic T cells through a small molecule-gated chimeric receptor. Science 2015; 350(6258): aab4077. doi: 10.1126/science.aab4077

35. Roybal KT, Rupp LJ, Morsut L, et al. Engineering T cells with customized therapeutic article engineering T cells with customized therapeutic esponse programs using synthetic notch receptors. Cell 2016; 167: 419–32.

36. Minutolo NG, Sharma P, Poussin M, et al. Quantitative control of gene-engineered T-cell activity through the covalent attachment of targeting ligands to a universal immune receptor. J Am Chem Soc 2020; 142: 6554–68.

37. Lynn RC, Weber EW, Sotillo E, et al. c-Jun overexpression in CAR T cells induces exhaustion resistance. Nature 2019; 576: 293–300.

38. Eyquem J, Mansilla-Soto J, Giavridis T, et al. Targeting a CAR to the TRAC locus with CRISPR/Cas9 enhances tumour rejection. Nature 2017; 543: 113–7.

39. Roth TL, Li PJ, Blaeschke F, et al. Pooled knockin targeting for genome engineering of cellular immunotherapies. Cell 2020; 181: 728–44.

40. Roth TL, Puig-Saus C, Yu R, et al. Reprogramming human T cell function and specificity with non-viral genome targeting. Nature 2018; 559: 405–9.

41. Tasian SK, Teachey DT, Li Y, et al. Potent efficacy of combined PI3K/mTOR and JAK or ABL inhibition in murine xenograft models of Ph-like acute lymphoblastic leukemia. Blood 2017; 129: 177–87.

42. Lee JC, Hayman E, Pegram HJ, et al. *In vivo* inhibition of human CD19-targeted effector T cells by natural T regulatory cells in a xenotransplant murine model of B cell malignancy. Cancer Res 2011; 71: 2871–81.

43. Sanmamed MF, Chester C, Melero I, Kohrt H. Defining the optimal murine models to investigate immune checkpoint blockers and their combination with other immunotherapies. Ann Oncol 2016; 27: 1190–8.

44. Holzapfel BM, Wagner F, Thibaudeau L, et al. Concise review: humanized models of tumor immunology in the 21st century: convergence of cancer research and tissue engineering. Stem Cells 2015; 33: 1696–704.

45. Kochenderfer JN, Yu Z, Frasheri D, et al. Adoptive transfer of syngeneic T cells transduced with a chimeric antigen receptor that recognizes murine CD19 can eradicate lymphoma and normal B cells. Blood 2010; 116: 3875–86.

46. Davila ML, Brentjens R. Chimeric antigen receptor therapy for chronic lymphocytic leukemia: what are the challenges? Hematol Oncol Clin North Am 2013; 27: 341–53.

47. Cheadle EJ, Hawkins RE, Batha H, et al. Natural expression of the CD19 antigen impacts the long-term engraftment but not antitumor activity of CD19-specific engineered T cells. J Immunol 2010; 184: 1885–96.

48. Cheadle EJ, Sheard V, Rothwell DG, et al. Differential role of Th1 and Th2 cytokines in autotoxicity driven by CD19-specific second-generation chimeric antigen receptor T cells in a mouse model. J Immunol 2014; 192: 3654–65.

49. Burga RA, Thorn M, Point GR, et al. Liver myeloid-derived suppressor cells expand in response to liver metastases in mice and inhibit the anti-tumor efficacy of anti-CEA CAR-T. Cancer Immunol Immunother 2015; 64: 817–29.

50. VanSeggelen H, Hammill JA, Dvorkin-Gheva A, et al. T cells engineered with chimeric antigen receptors targeting NKG2D ligands display lethal toxicity in mice. Mol Ther 2015; 23: 1600–10.

51. Chinnasamy D, Tran E, Yu Z, et al. Simultaneous targeting of tumor antigens and the tumor vasculature using T lymphocyte transfer synergize to induce regression of established tumors in mice. Cancer Res 2013; 73: 3371–80.

52. Pegram HJ, Lee JC, Hayman EG, et al. Tumor-targeted T cells modified to secrete IL-12 eradicate systemic tumors without need for prior conditioning. Blood 2012; 119: 4133–41.

53. Kunert A, Chmielewski M, Wijers R, et al. Intra-tumoral production of IL18, but not IL12, by TCR-engineered T cells is non-toxic and counteracts immune evasion of solid tumors. Oncoimmunology 2017; 7(1): e1378842. doi: 10.1080/2162402X.2017.1378842.

54. Chmielewski M, Abken H. CAR T cells releasing IL-18 convert to T-Bet high FoxO1 low effectors that exhibit augmented activity against advanced solid tumors. Cell Rep 2017; 21: 3205–19.

55. Hu B, Ren J, Luo Y, et al. Augmentation of antitumor immunity by human and mouse CAR T cells secreting IL-18. Cell Rep 2017; 20: 3025–33.

56. Zimmermann K, Kuehle J, Dragon AC, et al. Design and characterization of an all-in-one lentiviral vector system combining constitutive anti-G D2 CAR expression and inducible cytokines. Cancers (Basel) 2020; 12(2): e375. doi: 10.3390/cancers12020375

57. Adachi K, Kano Y, Nagai T, et al. IL-7 and CCL19 expression in CAR-T cells improves immune cell infiltration and CAR-T cell survival in the tumor. Nat Biotechnol 2018; 36: 346–51.

58. Rafiq S, Yeku OO, Jackson HJ, et al. Targeted delivery of a PD-1-blocking scFv by CAR-T cells enhances anti-tumor efficacy *in vivo*. Nat Biotechnol 2018; 36: 847–56.

59. Kuhn NF, Purdon TJ, van Leeuwen DG, et al. CD40 ligand-modified chimeric antigen receptor T cells enhance antitumor function by eliciting an endogenous antitumor response. Cancer Cell 2019; 35: 473–88.

60. Rodriguez-Garcia A, Lynn RC, Poussin M, et al. CAR-T cell-mediated depletion of immunosuppressive tumor-associated macrophages promotes endogenous antitumor immunity and augments adoptive immunotherapy. Nat Commun 2021; 12(1): e877. doi: 10.1038/s41467-021-20893-2

61. Hogan B. Manipulating mouse embryos. Cold Spring Harbor : Cold Spring Harbor Laboratory Press, 1994.

62. Eades-Perner AM, van der Putten H, Hirth A, et al. Mice transgenic for the human

carcinoembryonic antigen gene maintain its spatiotemporal expression pattern. Cancer Res 1994; 54: 4169–76.

63. Peat N, Gendler SJ, Lalani N, et al. Tissue-specific expression of a human polymorphic epithelial mucin (MUC1) in transgenic mice. Cancer Res 1992; 52: 1954–60.

64. Beavis PA, Henderson MA, Giuffrida L, et al. Targeting the adenosine 2A receptor enhances chimeric antigen receptor T cell efficacy. J Clin Invest 2017; 127: 929–41.

65. Chmielewski M, Hahn O, Rappl G, et al. T cells that target carcinoembryonic antigen eradicate orthotopic pancreatic carcinomas without inducing autoimmune colitis in mice. Gastroenterology 2012; 143: 1095–107.

66. Wang LX, Westwood JA, Moeller M, et al. Tumor ablation by gene-modified T cells in the absence of autoimmunity. Cancer Res 2010; 70: 9591–8.

67. Wang LX, Kang G, Kumar P, et al. Humanized-BLT mouse model of Kaposi's sarcoma-associated herpesvirus infection. Proc Natl Acad Sci U S A 2014; 111: 3146–51.

68. Bhattacharya-Chatterjee M, Saha A, Foon KA, Chatterjee SK. Carcinoembryonic antigen transgenic mouse models for immunotherapy and development of cancer vaccines. Curr Protoc Immunol 2008; 80: 20.8.1–12.

69. Brentjens RJ, Rivière I, Park JH, et al. Safety and persistence of adoptively transferred autologous CD19-targeted T cells in patients with relapsed or chemotherapy refractory B-cell leukemias. Blood 2011; 118: 4817–28.

70. Parkhurst MR, Yang JC, Langan RC, et al. T cells targeting carcinoembryonic antigen can mediate regression of metastatic colorectal cancer but induce severe transient colitis. Mol Ther 2011; 19: 620–6.

71. Eades-Perner AM, Zimmermann W. Carcinoembryonic antigen-transgenic mice: a model for tumor immunotherapy. Tumour Biol 1995; 16: 56–61.

72. Chan CHF, Stanners CP. Novel mouse model for carcinoembryonic antigen-based therapy. Mol Ther 2004; 9: 775–85.

73. Blat D, Zigmond E, Alteber Z, et al. Suppression of murine colitis and its associated cancer by carcinoembryonic antigen-specific regulatory T cells. Mol Ther 2014; 5: 1018–28.

74. Aranda F, Barajas M, Huarte E. Transgenic tumor models for evaluating CAR T-cell immunotherapies. Curr Protoc Pharmacol 2019; 86(1): e66. doi: 10.1002/cpph.66.

75. Brehm MA, Shultz LD, Greiner DL. Humanized mouse models to study human diseases. Curr Opin Endocrinol Diabetes Obes 2010; 17: 120–5.

76. Takenaka K, Prasolava TK, Wang JC, et al. Polymorphism in Sirpa modulates engraftment of human hematopoietic stem cells. Nat Immunol 2007; 8: 1313–23.

77. Smith DJ, Lin LJ, Moon H, et al. Propagating humanized BLT mice for the study of human immunology and immunotherapy. Stem Cells Dev 2016; 25: 1863–73.

78. Traggiai E, Chicha L, Mazzucchelli L, et al. Development of a human adaptive immune system in cord blood cell-transplanted mice. Science 2004; 304: 104–7.

79. Chicha L, Tussiwand R, Traggiai E, et al. Human adaptive immune system Rag2-/-gamma(c)-/- mice. Ann N Y Acad Sci 2005; 1044: 236–43.

80. Melkus MW, Estes JD, Padgett-Thomas A, et al. Humanized mice mount specific adaptive and innate immune responses to EBV and TSST-1. Nat Med 2006; 12: 1316–322.

81. Lan P, Tonomura N, Shimizu A, et al. Reconstitution of a functional human immune system in immunodeficient mice through combined human fetal thymus/liver and CD34+ cell transplantation. Blood 2006; 108: 487–92.

82. Wege AK, Melkus MW, Denton PW, et al. Functional and phenotypic characterization of the humanized BLT mouse model. Curr Top Microbiol Immunol 2008; 324: 149–65.

83. Norelli M, Camisa B, Barbiera G, et al. Monocyte-derived IL-1 and IL-6 are differentially required for cytokine-release syndrome and neurotoxicity due to CAR T cells. Nat Med 2018; 24: 739–48.

84. Arcangeli S, Bove C, Mezzanotte C, et al. CAR T cell manufacturing from naive/stem memory T lymphocytes enhances antitumor responses while curtailing cytokine release syndrome. J Clin Invest 2022; 132(12): e15080. doi: 10.1172/JCI150807

85. Page A, Laurent E, Nègre D, et al. Efficient adoptive transfer of autologous modified B cells: a new humanized platform mouse model for testing B cells reprogramming therapies. Cancer Immunol Immunother 2022; 71: 1771–5.

86. Lanitis E, Rota G, Kosti P, et al. Optimized gene engineering of murine CAR-T cells reveals the beneficial effects of IL-15 coexpression. J Exp Med 2021; 218(2): e20192203. doi: 10.1084/jem.20192203

PREDKLINIČNI MIŠJI MODELI PRI ADOPTIVNIH CELIČNIH TERAPIJAH RAKA

U. Rajčević, A. Smole

Izvleček: Napredne terapije na osnovi biotehnološko spremenjenih limfocitov T predstavljajo moderen pristop k imunoterapiji raka z uporabo genetsko spremenjenih limfocitov T. Do danes sta bili za zdravljenje hematoloških malignosti odobreni terapiji s himernimi antigenskimi receptorji usmerjenimi proti antigenoma CD19 in BCMA. Uspeh zdravljenja s celicami CAR-T pa ovirajo omejena učinkovitost, še posebej pri solidnih tumorjih in varnostna tveganja. Predklinične raziskave *in vivo*, ki so močno odvisne od zanesljivih mišjih modelov, so bile kritični dejavnik zgodbe o uspehu adoptivnih celičnih terapij in še vedno zagotavljajo neprecenljive podatke za razvoj naslednje generacije celičnih imunoterapij. V preglednem članku povzemamo štiri najpogostejše predklinične mišje modele: ksenografte, singenetske modele, imunokompetentne transgenske modele in humanizirane mišje modele. Vsi opisani modeli imajo svoje prednosti in slabosti in noben mišji model ne more do popolnosti preslikati situacije v človeškem pacientu zaradi medvrstnih razlik ter izjemne zapletenosti zdravljenja. Podatki iz literature kažejo na to, da lahko uporaba kombinacije mišjih modelov v predkliničnih in vivo raziskavah pred translacijo zdravljenja na ljudi v kliničnih poskusih pripomore k postopnemu izboljšanju kakovosti, varnosti in učinkovitosti zdravljenja in zagotovi bolj celostni nabor podatkov kot en sam model.

Ključne besede: mišji model; ksenograft; singenetski; transgenski; humanizirani; CAR-T; adoptivna celična terapija

Slov Vet Res 2022; 59 (4): 185–93
DOI 10.26873/SVR-1368-2022
UDC 636.8.09:616.831:616-001.1:614.86:616-089.17:005.585

Original Research Article

EVALUATION OF TRAUMA SCORING AND ENDOTHELIAL GLYCOCALYX INJURY IN CATS WITH HEAD TRAUMA

Kurtulus Parlak[1],*, Amir Naseri[2], Mustafa Yalcin[1], Eyup Tolga Akyol[3], Mahmut Ok[2], Mustafa Arican[1]

[1]Department of Surgery, [2]Department of Internal Medicine, Faculty of Veterinary Medicine, University of Selcuk, 42130, Konya, [3]Department of Surgery, Faculty of Veterinary Medicine, Balikesir University, 10145, Balikesir, Turkey

*Corresponding author, E-mail: kparlak@selcuk.edu.tr

Abstract: This study aim to evaluate the modified Glasgow Coma Scale (mGCS) and Animal Trauma Triage (ATT) scores, laboratory variables, and prognostic features of trauma-induced endothelial glycocalyx injury in cats with head trauma. Twenty-five cats with head trauma and 10 healthy cats were evaluated in this study. The enzyme-linked immunosorbent assay (ELISA) method was used to measure the levels of syndecan-1 and thrombomodulin in the serum of the 25 cats with head trauma (within 48 hours) and the 10 healthy cats. In addition, mGCS scores, ATT scores, laboratory values, syndecan-1 and thrombomodulin levels were compared between the cats that survived following treatment and the cats that did not survive despite treatment. Syndecan-1 and thrombomodulin levels were not statistically different between healthy cats and cats with head trauma. In the cats with head trauma, the mGCS scoring system was found to be more sensitive than the ATT scoring system. In conclusion, syndecan-1 and thrombomodulin levels did not yield statistically significant results in the cats with head trauma.

Key words: animal trauma triage; cat; head trauma; modified Glasgow coma scale; endothelial glycocalyx

Introduction

Head trauma is the most common injury in cats after extremity trauma (1). This type of trauma is commonly associated with motor vehicle accidents and high-rise syndrome (2, 3). Modified Glasgow Coma Scale (mGCS) and Animal Trauma Triage (ATT) are trauma-specific scoring systems used to classify trauma patients for prognostic purposes with quantification of injury severity (4–6). Trauma scores can facilitate the objective assessment of traumatized animals, and improve the outcome of treatments by predicting prognosis. The ATT score assesses six categories of body systems (perfusion, cardiac, respiratory, eye/muscle/integument, skeletal, and neurologic) and a scale of 0 to 3 for each category (0-slight or no injury, 3-severe injury), which contribute equally to the total score of 0 to 18 for prediction (5, 7). The mGCS was modified for veterinary use from the Glasgow Coma Scale, which has been described for humans with traumatic brain injury. This scale is based on the assessment of three categories, motor activity, brainstem reflexes, and level of consciousness. For each category, there is a scale from 1 to 6 (1-severely abnormal, 6-normal), with a lower total score indicating the more severe neurological deficits (4).

Recently, resuscitation efforts in severe trauma patients (humans, cats, dogs, etc.) have focused not only on restoring lost blood volume, but also on improving the recovery of inflammatory and coagulation responses, vascular permeability,

Received: 9 August 2021
Accepted for publication: 19 December 2022

and endothelial dysfunction (8, 9). In humans, head trauma and hemorrhagic shock are the most common causes of death in patients with trauma (10). In particular, hemorrhagic shock leads to systemic degradation of the endothelial glycocalyx layer, and these changes are thought to lead to traumatic endotheliopathy (EoT), a syndrome associated with high mortality (11–13). Therefore, biomarkers such as syndecan-1 and thrombomodulin have emerged for the assessment of coagulation and endothelial integrity (endothelial glycocalyx). In particular, hemorrhagic shock, sepsis, multiorgan failure, endothelial dysfunction, and damaged vascular permeability have been associated with increased morbidity and mortality (14, 15).

Overall, the purpose of this study is to investigate the mGCS and ATT scores as well as laboratory variables and markers of endothelial glycocalyx dysfunction for prognosis in cats with head trauma.

Materials and methods

Criteria for the selection of cases

Cats with a history of head injury (within 48 hours) that met clinical and neurologic examination criteria (mGCS and ATT scores) were included in the study. Delayed (over 48 hours), treated cases, and cats with polytrauma were excluded from the study.

Scoring methods

Clinical examinations of the cats with head injuries were performed by the same observer (KP) using the mGCS and the ATT scoring systems before analgesic medication was administered. On the mGCS, consciousness, brainstem reflexes, and motor activities were rated in three scoring categories: 3 to 8, "grave"; 9 to 14, "guarded"; 15 to 18, "good." As with the ATT assessment, body systems were rated in six categories (perfusion, cardiac, respiratory, eye/muscle/integument, skeletal, and neurologic) and scored on a scale of 0 to 3 in each category (4, 5).

CT imaging

A CT scan of the head was performed within 72 hours after trauma when the patient's condition had stabilized. The patient was premedicated with medetomidine hydrochloride (Domitor®, Zoetis) (0.08 ml/kg b.w., intramuscularly), and anesthesia was induced with propofol (Propofol %1, Fresenius Kabi) (4 - 6 mg/kg b.w., intravenously) and maintained with isoflurane (Forane®, Abbott) in oxygen via intubation tube. For the CT 120 kV, 100 mA, and 2 mm cross-sectional thickness were selected and performed in helical cranial scanning mode. CT was used for head bone assessment only.

Blood sample collection

On admission, 2 ml of blood was collected by jugular venipuncture. Depending on the clinical condition of the cases, blood analyzes were repeated during the monitoring process. One part (0.5 ml) of the collected sample was immediately used for venous blood gas analysis, and the rest for complete blood count (CBC) and biochemistry (serum) analysis. Serums were stored at – 80 °C and thawed immediately before ELISA (enzyme-linked immunosorbent assay) analysis.

Blood gases and complete blood count

Venous blood gas analysis, which includes pH, partial pressure of carbon dioxide (pCO_2), partial pressure of oxygen (pO_2), venous oxygen saturation (sO_2), lactate, sodium (Na), calcium (Ca), chloride (Cl), potassium (K), glucose, base excess (BE), and bicarbonate (HCO_3) was performed using an automated blood gas analyzer (ABL 90 Flex, Radiometer, USA). Blood counts including total leukocytes, lymphocytes, monocytes, granulocytes, erythrocytes, hematocrit (HCT), hemoglobin (Hgb), and platelets were obtained using an automated cell counter (MS4e, Melet Schlosing Laboratories, France).

Measuring syndecan-1 and thrombomodulin by the ELISA method

Serum concentrations of syndecan-1 and thrombomodulin were measured according to the manufacturer's protocol using the feline syndecan-1 commercial sandwich ELISA kit (catalog number: MBS1603385, USA) and the feline thrombomodulin commercial ELISA kit (catalog number: MBS1603383, USA) with an ELISA reader (Biotek 800TS, BioSPX, The Netherlands). Intra-

assay coefficients, inter-assay coefficients, and minimum detectable concentrations were < 8%, < 10%, and 0.025 ng/ml for syndecan-1 cat, < 8%, < 10%, and 0.017 ng/ml for thrombomodulin.

Treatment protocol

The treatment protocol was applied to the cats with head trauma immediately after scoring and blood collection, and this protocol was repeated depending on the condition of the patients in the intensive care unit. The goals of the treatment protocol were based on the stimulation of circulation and oxygen delivery to vital organs. Fluid therapy with crystalloid solution 0.9% NaCl (60 ml/kg/hour, b.w., intravenously), osmotic diuretic mannitol (20% Mannitol, Polifarma) (2 g/kg b.w., intravenously, in 15 minutes), oxygen therapy (flow rate 100 ml/kg/min, intranasal or flow-by, oxygen cage), butorphanol (Butomidor®, Richter Pharma) (0.4 mg/kg b.w., subcutaneously) for analgesia, levetiracetam (Keppra®, UCB Pharma) (40 mg/kg b.w, intramuscularly) for anticonvulsant therapy, and nutrition (oral feeding or nasogastric tube feeding and esophageal feeding) were performed in cats with head trauma.

Statistical methods

To determine if the variables had a normal distribution, the Shapiro-Wilk test was used. In addition, parametric data were analyzed with the Student t-test (as mean ± standard deviation (SD)), nonparametric data were analyzed with the Mann-Whitney U test (as median (min/max)), and linear regression analysis was performed to determine the independent predictors of mortality. The prognostic value of serum endothelial biomarkers, mGCS, and hematologic variables was also evaluated using a receiver operating characteristic curve (ROC) to determine the prognostic cut-off values for best discrimination between survivors and nonsurvivors. Finally, the Kaplan-Meier survival curve from GCS was constructed. Overall, the statistical significance was $P < 0.05$, and data analysis was performed using SPSS statistical software.

Results

The animals in this study consisted of 25 cats with acute head trauma (24 mixed-breed and one British Shorthair; 14 males and 11 females; mean age, 13.4 (1-48) months) and 10 healthy cats (control group) (10 mixed-breed; 6 females and 4 males; mean age, 15.2 (8-28) months).

Of the 25 cats with head trauma, 5 cats (20%) had trauma due to high-rise syndrome and 20 cats (80%) had trauma due to motor vehicle accidents. In addition, 8 cats (32%) had severe head trauma (mGCS score 3 - 8, "grave"), 10 cats (40%) had moderate head trauma (mGCS score 9 - 14, "guarded"), and 7 cats (28%) had mild head trauma (mGCS score 15 - 18, "good"). Compared with the mGCS scores, the ATT scores ranged from 5 - 14 (mean 9) in the cats with severe trauma, from 4 - 12 (mean 7.5) in the cats with moderate trauma, and 2 - 7 (mean 4.7) in the cats with mild trauma (Table 1).

CT scan was performed in 15 / 25 cats with head trauma. The CT could not be performed in 8 cats because of their poor clinical condition and in 2 cats because their owners did not give permission. There were no abnormal findings in 2 / 15 cats. In addition, in 1 of the cats in which a CT scan was not performed, separation of the mandibular symphysis was clinically detected and treated. Regarding the CT findings of the other cats, separation of the symphysis mandible (n = 8), temporomandibular joint (TMJ) fracture (n = 5), os temporale fracture (n = 1), os zygomaticus fracture (n = 2), and separation of the palatal bone (n = 8) were observed (Table 1). There were no complications related to anesthesia during the CT scans.

Finally, 12 of the 25 cats with head trauma were discharged after treatment (the average treatment time for discharged cats is 96 hours), whereas the remaining 13 cats died (no cat was euthanized). In this context, hematologic values, trauma scores (mGCS, ATT), and endothelial glycocalyx layer data (syndecan-1, thrombomodulin) were statistically compared between non-surviving and surviving cats (Figure 1) (Table 2).

Linear regression analysis showed that mGCS, K^+, HCO_3, WBC, and Hb were independent risk factors for mortality in the head trauma group, whereas ROC analysis for the benefit of mGCS in discriminating between surviving and non-surviving cats yielded an area under the curve of 0.76 (p = 0.028, 95% CI = 0.569-0.950) (Figure 2). Furthermore, the optimal cut-off point of 14.50 for the mGCS corresponded to a sensitivity of 76% and a specificity of 70% for predicting

Table 1: Trauma scores and findings on cases

Case	Trauma Type	CT Results	mGCS	ATT	Survivors/ Non-survivors
Cat 1	HRS	TMJ Fracture (Left) Os zygomaticus fracture	14	8	N
Cat 2	MVA	CT not applied	17	2	N
Cat 3	MVA	TMJ Fracture (Right)	16	7	N
Cat 4	MVA	CT not applied	5	9	Y
Cat 5	MVA	CT not applied	6	9	N
Cat 6	MVA	CT not applied	3	5	N
Cat 7	MVA	CT not applied	4	6	N
Cat 8	MVA	Separation of the symphysis mandible	18	7	Y
Cat 9	MVA	TMJ fracture (Left) Separation of the symphysis mandible	16	5	Y
Cat 10	MVA	Separation of the palatal bone	16	3	Y
Cat 11	MVA	TMJ Fracture (Right) Separation of the symphysis mandible Separation of the palatal bone	3	11	N
Cat 12	MVA	Os temporale fracture Separation of the palatal bone	12	5	Y
Cat 13	MVA	Separation of the symphysis mandible Separation of the palatal bone	15	7	Y
Cat 14	HRS	Different structure not seen	14	9	N
Cat 15	MVA	Separation of the symphysis mandible	14	9	N
Cat 16	MVA	Separation of the symphysis mandible Separation of the palatal bone	10	6	Y
Cat 17	MVA	TMJ fracture (Right) Separation of the palatal bone	11	7	N
Cat 18	MVA	Os zygomaticus fracture Separation of the symphysis mandible Separation of the palatal bone	5	10	N
Cat 19	HRS	Different structure not seen	13	8	N
Cat 20	MVA	Separation of the palatal bone	9	4	Y
Cat 21	MVA	CT not applied	6	7	Y
Cat 22	HRS	CT not applied	18	2	Y
Cat 23	MVA	CT not applied	13	7	Y
Cat 24	MVA	CT not applied	13	7	Y
Cat 25	HRS	CT not applied	4	14	N

HRS: High-Rise Syndrome, TMJ: Temporomandibular Joint, MVA: Motor vehicle accidents, mGCS: Modified Glasgow Coma Scale, ATT: Animal Trauma Triage, Y: Survivors, N: Non-survivors

mortality. Finally, a probability curve for the mGCS score showed a 72% probability of nonsurvival at a score of 6 and a 56% probability of non-survival at a score of 13, whereas a mentation score of 3 showed a 92% probability of nonsurvival (Figure 3).

Discussion

The primary causes of head injuries are traffic accidents, followed by high-rise syndrome (3). Of the 25 cats with head trauma in the present study, 80% were due to motor vehicle accidents, whereas 20% were due to high-rise syndrome, which is consistent with the results of previous studies.

Some researchers have evaluated different scoring systems, such as the mGCS and ATT scoring systems, as prognostic indicators of trauma in cats and dogs (4, 7, 16). For instance, Lapsley et al (7) studied the mGCS and ATT scoring systems in 711 cats with trauma.

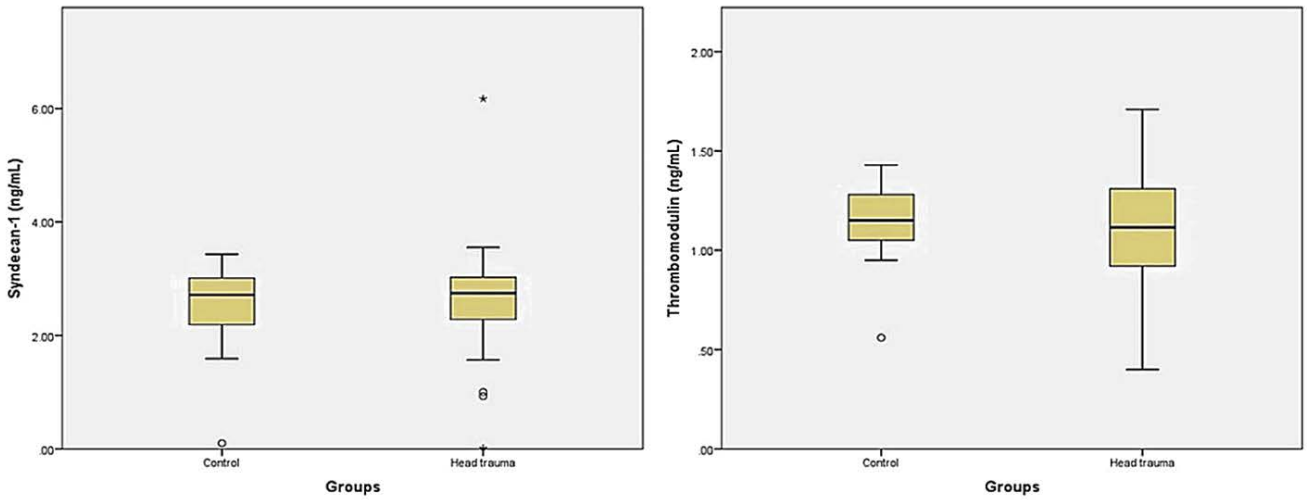

Figure 1: Comparison of the syndecan-1 (left) and thrombomodulin (right) levels of healthy cats and cats with head trauma

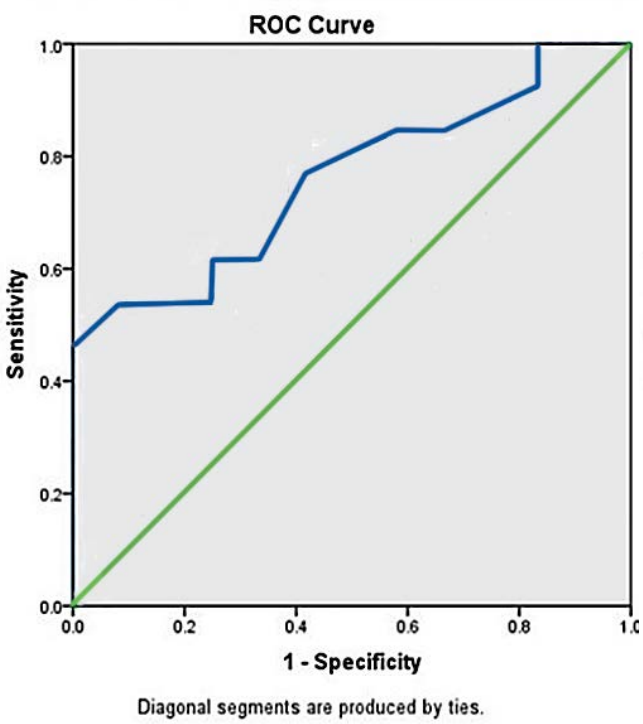

Figure 2: Receiver operating characteristic curve (ROC) analysis for the utility of the modified Glasgow Coma Scale to discriminate between surviving and nonsurviving cats yielded an area under the curve of 0.76 (p = 0.028, 95% CI = 0.569 - 0.950)

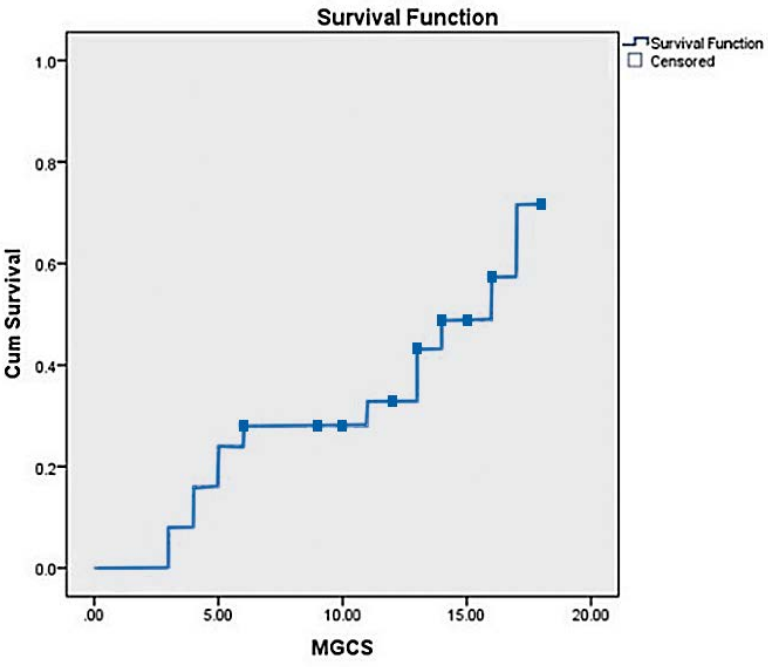

Figure 3: A probability curve for the modified Glasgow Coma Scale score showed a 72% probability of nonsurvival at a score of 6 and a 56% probability of nonsurvival at a score of 13, whereas a mentation score of 3 showed a 92% probability of nonsurvival

However, when they limited the study to patients with head trauma, they found that there was no significant difference in differential capacity between the two scoring systems.

In a related study, Sharma and Holowaychuk (16) performed prognostic assessments of 72 dogs with head trauma and found that both scoring systems, particularly the mGCS, had prognostic value. In addition, Platt et al (4) reported that the mGCS can be evaluated as prognostic data in dogs with head trauma. In the present study, when the mGCS and ATT scores of the non-surviving and

Table 2: Mean trauma scores (mGCS, ATT), endothelial glycocalyx layer data (syndecan-1, thrombomodulin), and hematologic values were statistically compared between nonsurviving and surviving cats

Parameter	Survivors (n: 12)	Non-survivors (n: 13)	P-value
mGCS	14 (6 - 18)	6 (3 - 17)	0.026
ATT	6 (2 - 12)	8 (2 - 14)	0.110
Syndecan-1 (ng/ml)	2.49 ± 0.94	2.59 ± 1.34	0.827
Thrombomodulin (ng/ml)	1.14 ± 0.30	1.02 ± 0.29	0.319
pH	7.32 ± 0.49	7.26 ± 1.12	0.076
pCO_2 (mmHg)	35.02 ± 5.90	35.56 ± 5.73	0.818
pO_2 (mmHg)	36.54 ± 6.18	34.06 ± 4.01	0.255
sO_2 (%)	47.62 ± 14.17	44.38 ± 8.64	0.503
cK^+ (mmol/L)	3.72 ± 0.58	3.19 ± 0.68	0.047
cNa^+ (mmol/L)	159.58 ± 3.08	159.53 ± 9.68	0.988
cCa^+ (mmol/L)	0.87 ± 0.19	0.81 ± 0.22	0.452
cCl^- (mmol/L)	120 (116 - 125)	121 (92 - 181)	0.205
cGlu (mg/dL)	209.58 ± 52.64	212.76 ± 66.50	0.895
cLac (mmol/L)	3.00 ± 1.75	2.13 ± 1.34	0.182
cBase (Ecf) (mmol/L)	-7.70 ± 1.55	- 10.21 ± 4.05	0.055
$cHCO_3^-$ (mmol/L)	17.90 ± 1.13	16.05 ± 2.63	0.034
WBC (cells/ml)	26.36 ± 11.65	15.79 ± 9.22	0.021
LYM (cells/ml)	7 (1 - 18)	5 (2 - 15)	0.247
MON (cells/ml)	1 (0.14 - 12)	0.99 (0.51 - 4)	0.437
GRA (cells/ml)	14.12 ± 8.28	8.67 ± 7.80	0.105
RBC ($x10^3$ cells/ml)	10.66 ± 1.93	8.72 ± 2.72	0.051
Hct (vol%)	44.07 ± 9.65	36.12 ± 11.26	0.070
Hgb (g/dl)	12 (8 - 45)	10 (7 - 16)	0.022
Platelets (cells/ml)	199.58 ± 101.84	214.76 ± 76.02	0.679

surviving cats were compared, it was found that the mGCS was statistically more prominent in head trauma in terms of prognosis. It was also suggested that the lack of statistical prognostic value of the ATT system was since this study focused only on cats with isolated head trauma and not on cats with polytrauma. It is important to note that the ATT scoring system generally assesses all body systems, including the musculoskeletal system, whereas the mGCS provides a more specific assessment of the central nervous system.

In general, CT scans are used to diagnose hematomas, contusions, hernias, and cerebral ischemia, especially fractures in patients with head trauma (17, 18). It has also been used in the determination of craniomaxillofacial fractures in cats with head trauma. Recent studies report that mandibular fractures, particularly the separation of the mandibular symphysis and TMJ fractures, are the most common injuries diagnosed with CT in cats after head trauma (19, 20). In addition, Tundo et al (20) stated that fractures involving the skull in cats after head trauma had a common and predictable distribution pattern in the midface (nose, maxilla, intermaxillary suture, orbit, nasopharynx, and zygomatic arch), with a high incidence of TMJ fractures. According to the CT scans in this study, the most common injuries were the separation of the mandibular symphysis, separation of the palatal bone, and TMJ fractures. The results are consistent with those of recent studies (19, 20). It is important to point out that one of the main problems that limited our CT imaging method was the inadequacy of the older generation of equipment, which prevented us from scanning thinner sections and obtaining detailed views of small structures.

Some retrospective studies have been performed to determine the association between

the severity of injury and hyperglycemia in cats and dogs with head trauma. Thus, some studies have indicated that cats and dogs with head trauma may have hyperglycemia, the extent of which is related to the severity of head trauma (16, 21). However, in the present study, no statistically significant difference was found between hyperglycemia and mortality, based on the statistical analyses between non-surviving and surviving cats with head trauma. However, blood glucose levels were found to be higher than normal in the cats with head trauma.

In this study, Hgb, HCO_3, and K^+ levels decreased below normal values on laboratory examination of non-surviving cats at the time of admission. Their white blood cell counts, although at normal levels, were lower than those of the surviving cats. In addition, a decrease in venous pO_2 was observed in all cats with head trauma, including both non-surviving and surviving cats. Previous studies have shown that such a decrease, especially in dogs with head trauma, is due to impaired hemodynamic stability, which may lead to secondary brain damage (16). According to the data of the present study, this situation may also occur in cats with head trauma.

Previous studies have shown an association between the detachment of glycocalyx components (syndecan-1 and thrombomodulin) and increased morbidity and mortality (22, 23). A previous study by Albert et al (24) examined the effects of endothelial damage on mortality by focusing on syndecan-1 and thrombomodulin levels in human patients with a head injury. They found that there was no significant increase in syndecan-1 levels associated with traumatic brain injury (TBI), which is a determinant of endothelial glycocalyx damage, and no significant change in thrombomodulin levels. However, they found a significant association between increased syndecan-1 levels and mortality (24). In a related study, Rodriguez et al (25) examined endothelial glycocalyx dysfunction using syndecan-1 and thrombomodulin levels in isolated TBI, polytraumatic TBI, and TBI-free trauma patients. They determined that syndecan-1 levels were highest in the polytraumatic TBI group, whereas they were lowest in the isolated TBI group. They also pointed out that thrombomodulin levels, although higher than normal, were similar in the three groups. In addition, the isolated TBI patients reported experiencing less glycocalyx destruction, as measured by their circulating syndecan-1 levels. Again, increased syndecan-1 concentrations were associated with increased 72 hours mortality in the isolated TBI patients (25).

Because there have been no previous studies of syndecan-1 and thrombomodulin levels in cats with head trauma, the results of the present study were compared with those of human studies. According to studies, the syndecan-1 levels were increased in the endothelial glycocalyx damage of patients with head trauma, and this was more strongly associated with mortality than the increase in thrombomodulin levels. However, in our study, there was no statistically significant result related to syndecan-1 and thrombomodulin levels in the cats that did not survive after head trauma. Therefore, the results of this study differ from those of human studies and the use of different biomarkers related to endothelial glycocalyx injury may lead to more efficient results.

Our study had several limitations: 1) the study population was relatively small, and reevaluation of the hypothesis of endothelial glycocalyx damage in larger sample populations is warranted. 2) Histopathological examinations were not performed on cats that did not survive after head trauma.

Conclusion

This was the first study to perform prognostic assessments based on the mGCS and ATT scoring systems and endothelial glycocalyx layers in cats with head trauma. Overall, no statistically significant difference was found between the syndecan-1 and thrombomodulin levels of the healthy cats and those of the cats with head trauma. In addition, linear regression analysis showed that the mGCS, potassium, bicarbonate, white blood cell, and hemoglobin levels were independent mortality factors in the head trauma group. Although the mGCS and ATT scoring systems are the most common scoring systems used to assess cats with trauma, the former is believed to be one step ahead of the latter. However, the markers syndecan-1 and thrombomodulin were not found to be useful for prognosis or choice of treatment options in cats with head trauma.

Acknowledgements

Supported by the Coordination of Scientific Research Projects of Selçuk University (BAP) (No. 19401043). The authors thank N. Zamirbekova and all staff from the Department of Surgery for animal care.

Ethical approval: This study was approved by the Ethics Committee (03/2019) of the Faculty of Veterinary Medicine and Experimental Animal Production and Research Centre, Selçuk University, Turkey. Informed owner consent was also obtained from the owners and the ethical guidelines of the institution were followed.

References

1. Kolata RJ. Trauma in dogs and cats: an overview. Vet Clin North Am Small Anim Pract 1980; 10: 515–22.

2. Rochlitz I. Study of factors that may predispose domestic cats to road traffic accidents: Part 2. Vet Rec 2003; 153(19): 585–8.

3. Vnuk D, Pirkić B, Matičić D, et al. Feline high-rise syndrome: 119 cases (1998–2001). J Feline Med Surg 2004; 6: 305–12.

4. Platt SR, Radaelli ST, McDonnell JJ. The prognostic value of the modified Glasgow coma scale in head trauma in dogs. J Vet Intern Med 2001; 15: 581–4.

5. Rockar RA, Drobatz KS, Shofer FS. Development of a scoring system for the veterinary trauma patient. J Vet Emerg Crit Care 1994; 4: 77–83.

6. Shores A. Craniocerebral trauma. In: Kirk RW, ed. Current veterinary therapy X. Philadelphia : WB Saunders, 1983: 547–54.

7. Lapsley J, Hayes GM, Sumner JP. Performance evaluation and validation of the Animal Trauma Triage score and modified Glasgow coma scale in injured cats: a Veterinary Committee on Trauma registry study. J Vet Emerg Crit Care 2019; 29: 478–83.

8. Midwinter MJ, Woolley T. Resuscitation and coagulation in the severely injured trauma patient. Philos Trans R Soc B Biol Sci 2011; 366: 192–203.

9. Pierce A, Pittet JF. Inflammatory response to trauma: implications for coagulation and resuscitation. Curr Opin Anaesthesiol 2014; 27: 246–52.

10. Oyeniyi BT, Fox EE, Scerbo M, Tomasek JS, Wade CE, Holcomb JB. Trends in 1029 trauma deaths at a level 1 trauma center: Impact of a bleeding control bundle of care. Injury 2017; 48: 5–12.

11. Chignalia AZ, Yetimakman F, Christiaans SC, et al. The glycocalyx and trauma: a review. Shock 2016; 45: 338–48.

12. Johansson PI, Stensballe J, Ostrowski SR. Shock induced endotheliopathy (SHINE) in acute critical illness: a unifying pathophysiologic mechanism. Crit Care 2017; 21(1): e25. doi: 10.1186/s13054-017-1605-5.

13. Johansson PI, Henriksen HH, Stensballe J, et al. Traumatic endotheliopathy: a prospective observational study of 424 severely injured patients. Ann Surg 2017; 265: 597–603.

14. Lee WL, Slutsky AS. Sepsis and endothelial permeability. N Engl J Med 2010; 363: 689–91.

15. Haywood-Watson RJ, Holcomb JB, Gonzalez EA, et al. Modulation of syndecan-1 shedding after hemorrhagic shock and resuscitation. PLoS One 2011; 6(8): e23530. doi: 10.1371/journal.pone.0023530.

16. Sharma D, Holowaychuk MK. Retrospective evaluation of prognostic indicators in dogs with head trauma: 72 cases (January–March 2011). J Vet Emerg Crit Care 2015; 25: 631–9.

17. Kolias AG, Guilfoyle MR, Helmy A, Allanson J, Hutchinson PJ. Traumatic brain injury in adults. Pract Neurol 2013; 13: 228–35.

18. Currie S, Saleem N, Straiton JA, Macmullen-Price J, Warren DJ, Craven IJ. Imaging assessment of traumatic brain injury. Postgrad Med J 2016; 92: 41–50.

19. Knight R, Meeson RL. Feline head trauma: a CT analysis of skull fractures and their management in 75 cats. J Feline Med Surg 2019; 21: 1120–6.

20. Tundo I, Southerden P, Perry A, Haydock RM. Location and distribution of craniomaxillofacial fractures in 45 cats presented for the treatment of head trauma. J Feline Med Surg 2019; 21: 322–8.

21. Syring RS, Otto CM, Drobatz KJ. Hyperglycemia in dogs and cats with head trauma: 122 Cases (1997–1999). J Am Vet Med Assoc 2001; 218: 1124–9.

22. Rahbar E, Baer LA, Cotton BA, Holcomb JB, Wade CE. Plasma colloid osmotic pressure is an early indicator of injury and hemorrhagic shock. Shock 2014; 41: 181–7.

23. Torres Filho I, Torres LN, Sondeen JL, Polykratis IA, Dubick MA. In vivo evaluation of venular glycocalyx during hemorrhagic shock in rats using intravital microscopy. Microvasc Res 2013; 85: 128–33.

24. Albert V, Subramanian A, Agrawal D, Pati H, Gupta S, Mukhopadhyay A. Acute traumatic endotheliopathy in isolated severe brain injury and its impact on clinical outcome. Med Sci 2018; 6(1): e5. doi: 10.3390/medsci6010005.

25. Rodriguez GE, Cardenas JC, Cox CS, et al. Traumatic brain injury is associated with increased syndecan-1 shedding in severely injured patients. Scand J Trauma Resusc Emerg Med 2018; 26(1): e102. doi: 10.1186/s13049-018-0565-3

VREDNOTENJE SISTEMA OCENJEVANJA TRAVME IN POŠKODB ENDOTELIJSKEGA GLIKOKALIKSA PRI MAČKAH S POŠKODBO GLAVE

K. Parlak, A. Naseri, M. Yalcin, E. T. Akyol, M. Ok, M. Arican

Izvleček: Namen te študije je bil ovrednotiti spremenjeno glasgowsko lestvico kome (angl. Glasgow Coma Scale, GCS) in ocene ATT (Animal Trauma Triage), laboratorijske spremenljivke in prognostične značilnosti s travmo povzročene poškodbe endotelijskega glikokaliksa pri mačkah s poškodbo glave. V študijo je bilo vključenih 25 mačk s poškodbo glave in 10 zdravih mačk. Ravni sindekana-1 in trombomodulina v serumu 25 mačk s poškodbo glave (v 48 urah) in 10 zdravih mačk smo merili z encimsko imunoadsorpcijsko preiskavo (ELISA). Ocene mGCS, ocene ATT, laboratorijske vrednosti ter ravni sindekana-1 in trombomodulina smo primerjali med mačkami, ki so po zdravljenju preživele, in mačkami, ki kljub zdravljenju niso preživele. Vrednosti sindekana-1 in trombomodulina se med zdravimi mačkami in mačkami s poškodbo glave niso statistično razlikovale. Pri mačkah s poškodbo glave se je sistem točkovanja mCGS izkazal za občutljivejšega od sistema točkovanja ATT. Zaključili smo, da vrednosti sindekana-1 in trombomodulina pri mačkah s poškodbo glave niso statistično pomembne.

Ključne besede: triaža poškodb živali; mačka; poškodba glave; spremenjena glasgowska lestvica kome; endotelijski glikokaliks

Slov Vet Res 2022; 59 (4): 195–209
DOI 10.26873/SVR-1591-2022
UDC 615.9:546.81:616-091.8:615.035:547.458.88:599.323.452

Original Research Article

PECTIN IMPROVES HEMATO-BIOCHEMICAL PARAMETER, HISTOPATHOLOGY, OXIDATIVE STRESS BIOMARKERS, CYTOKINES AND EXPRESSION OF HEPCIDIN GENE IN LEAD INDUCED TOXICITY IN RATS

Sabry M. El-Bahr[1,2]*, Saad Al-Sultan[1,3], Ahlam F. Hamouda[4], Shimaa. A. E. Atwa[5], Seham Y. Abo-Kora[6], Aziza A. Amin[7], Saad Shousha[1,8], Sameer Alhojaily[1], Aymmen Alnehas[9], Rabab R. Elzogby[10]

[1]Department of Biomedical Sciences, [3]Department of Public Health, [9]Department of Clinical Sciences, College of Veterinary Medicine, King Faisal University, Al-Ahsa, 31982, Saudi Arabia, [2]Department of Biochemistry, Faculty of Veterinary Medicine, Alexandria University, Alexandria, 21523, Egypt, [4]Department of Forensic Medicine and Toxicology, Teaching Hospital, [5]Department of Biochemistry, [6]Department of Pharmacology, [7]Department of Histopathology, [8]Department of Physiology, Faculty of Veterinary Medicine, Benha University, Benha, 13736, [10]Department of Pharmacology, Faculty of Veterinary Medicine, NewVally University, Egypt

*Corresponding author, E-mail: selbahar@kfu.edu.sa

Abstract: Publications concerning the protective effect of pectin against lead induced toxicity in rats are not available. In order to study such effect, 40 male rats were divided into 3 groups. The first group was contained 10 rats that kept as control group. The second group was contained 10 rats that received pectin at dose of 100 mg/kg BW during experimental period (8 weeks). The third group was contained 20 rats that received 400mg/kg BW of lead acetate daily for 4 weeks then divided into two subgroups (3A and 3B). Subgroup 3A contained 10 rats that still receive lead acetate in the same dosage whereas, subgroup B co-treated with lead acetate and pectin daily for another 4 weeks. Blood samples were collected after 2, 4 and 8 weeks from the start of the experiment. Liver, kidney and bone marrows were collected only at the end of the experiment. Lead acetate induced anemia only after 4 weeks of administration as reflected on decreased values of Hb, PCV, MCV, MCH and MCHC. These indices remained at lower levels in lead acetate treated groups until the end of the experiment. Concentrations of serum ferritin, iron, total antioxidant capacity (TAC) and reduced glutathione (GSH) and the expression of hepatic hepcidin gene were decreased significantly in lead acetate intoxicated rats compared to control. Activities of ALT and AST and concentrations of urea, creatinine, Nitric oxide (NO), TNF-α, IL-6, total iron binding capacity (TIBC) and lead were increased significantly in lead acetate intoxicated group compared to control. Hepatic degeneration and hemorrhage, renal lytic necrosis and apoptosis of myeloid cells were most prominent changes in lead intoxicated rats. Lead acetated related changes were improved by co-treatment with pectin however; normal control values have not been achieved. Conclusively, pectin is recommended to protect against lead acetate toxicity in rats.

Key words: lead acetate; toxicity; pectin; hepcidin; oxidative stress biomarkers; histopathology

Introduction

One of the most serious environmental medicine issues is lead poisoning. Lead contamination in the environment caused by industrial lead production and metal recycling (1). Due to its harmful cumulative action in the environment, lead can affect all biological systems by exposure from multiple sources such as air, water, and food. Lead has the ability to migrate up the food chain, causing harm to humans and other animals. Lead induced microcytic hypochromic anemia in mammals due to its interaction with iron and copper metabolism (2). Lead may disrupt the integrity of the RBC membrane, making it more fragile, resulting in a disorder of red blood cell metabolism in the bone marrow or mature erythrocytes, inhibit the enzyme ferrochelatase and reducing iron (Fe) incorporation into heme and disrupting heme synthesis (3).

Received: 22 September 2022
Accepted for publication: 13 October 2022

Lead exposure has been observed to reduce serum iron and transferrin saturation levels in rats (4). Lead acetate has hepatoxic effect which increase hepatocyte permeability in rats. The damaged hepatocyte cell membrane of hepatocytes leading to escape of liver enzymes to blood. Lead toxicity produces an increase in cellular basal metabolic rate, irritability, and destructive alteration of liver cells due to its oxidative effect (5). Oral dose of lead acetate caused a significant rise in blood urea and serum creatinine in rats (6). The main mechanism responsible for lead toxicity is oxidative stress. This type of stress causes changes in the composition of fatty acids in cells membrane (affecting processes such as exocytosis and endocytosis, as well as signal transduction processes). The production of reactive oxygen species (ROS), the activation of lipid peroxidation, and the depletion of antioxidant reserves are all factors that contribute to lead exposure (3, 7). Hepcidin gene expression is reduced after experimentally induced anemia and hypoxia, which could explain the increased (Fe) release from reticuloendothelial cells and higher (Fe) absorption normally observed in these conditions, suggesting hepcidin involvement in anemic states. Lead has also been found to prevent (Fe) from being transferred from endosomes to the cytoplasm (8). Hepcidin expression was found to be lower in people with anemia of chronic disorders (ACD) and in mammalian models that resembled ACD (9, 10). In patient and mammals with (ACD), iron deficiency anemia, serum hepcidin levels and/or liver mRNA expression were both decreased considerably (9). Additionally, Hypoxia may diminish hepcidin expression while increasing serum iron and transferrin saturation, allowing massive erythropoiesis to compensate for tissue hypoxia (11). Pectin is a galacturonic acid polymer found mostly in plant walls. It can be isolated from fruit pips, apple pulp, and peal (12). Pectin rich in galacturonic acid (GalA) are effective at chelating heavy metals (13). Pectin's ability to chelate metals in the digestive system and inhibit absorption while aiding their removal in the faces, toxic metal absorption and bioaccumulation were reduced with its administration (14). Oral administration of pectin resulted in decrease lead absorption (15). In industrial settings, commercial apple pectin is an excellent agent for preventing lead incorporation (16). The goal of this work was to evaluate the effect of pectin on hemato-biochemical parameter, histopathology, oxidative stress biomarkers, cytokines and expression of Hepcidin gene in lead intoxicated rats.

Materials and methods

Chemicals

Lead acetate obtained from Al Gomhoria company, Egypt. Pectin obtained from Sigma Company, Egypt.

Experimental animals and design

This experiment was carried out according to the guidelines of the Institutional Animal Ethics Committee, Benha University, Egypt, and Approval (Permission # BUFVTM 05-12-21**).** Forty male albino rats were purchased from Lab Animal House at Vet College Benha University; their average weight was (160±10g). They kept in well-ventilated metal cages throughout the study and acclimatized for one week at a temperature of 18-24°C with 12 hours of light and darkness, on normal feed diet and water ad libitum. The experimental design illustrated obviously at Table 1. This design showed that, 40 male rats were divided into 3 groups. The first group was contained 10 rats that kept as control group and received normal physiological saline daily during experimental period (8 weeks). The second group was contained 10 rats that received pectin at dose of 100 mg/kg BW (17) during experimental period (8 weeks). The third group was contained 20 rats that received 400mg/kg BW of lead acetate daily (18) for 4 weeks then divided into two subgroups (3A and 3B). Subgroup 3A contained 10 rats that still receive lead acetate in the same dosage whereas, subgroup B co-treated with lead acetate and pectin daily for another 4 weeks. Blood samples were collected after 2, 4 and 8 weeks from the start of the experiment. The whole blood was used or the detection of hematological indices (Hb, PCV, MCV, MCH and MCHC). The obtained serum was used for the estimation of the activity of ALT and AST and the concentration of urea, creatinine, ferritin, iron, TIBC TAC, GSH, NO, TNF-α, IL-6 and lead. Liver, kidney and bone marrows collected only at the end of the experiment and subjected to histopathological examination. Portion of liver tissues was frozen by liquid nitrogen until used for detection of expression of hepatic hepcidin gene.

Table 1: The experimental design of the study

Time	Samples	Parameters measured	Groups			
			Group 1	Group 2	Group 3	
After 2 weeks	blood	Hb, RBCs, PCV, MCV, MCH, MCHC	✓	✓	✓	
After 4 weeks	blood	Hb, RBCs, PCV, MCV, MCH, MCHC,	✓	✓	✓	
					3A	3B
After 8 weeks	Blood, serum, liver, kidney, bone marrow	Hb, RBCs, PCV, MCV, MCH, MCHC, Basophilic Stippling cell, Ferritin, Iron, TIBC, AST, ALT, urea, creatinine, TAC, GSH, NO, TNF-α, IL-6, lead, Histopathology	✓	✓	✓	✓

Assessment of Complete blood count

Assessing of complete blood count was performed using an electronic cell counter (VetScan HM5 Hematology system, Abaxis, Inc., Union City, CA, USA).

Assessment of liver and kidney function tests and iron profile

Activities of ALT and AST were performed as described earlier (19). Serum urea and creatinine were performed as described previously (20, 21), respectively. Serum iron, ferritin and Total iron Binding Capacity (TBIC) were performed as described earlier (22, 23, 24), respectively.

Assessment of serum oxidative stress biomarker and cytokines concentrations

The total antioxidant capacity (TAC), reduced glutathione (GSH) and nitric oxide (NO) were performed as described in previous researches (25, 26, 27), respectively. TNF-α and IL-6 concentrations were determined by using ELISA kit that described earlier (28).

Detection of lead residues in blood

Detection of lead residues in blood was performed as described earlier (29). Briefly, 1ml whole blood was measured into clean test tubes, followed by 1 ml concentrated nitric acid containing 0.1 percent triton-100, which was mixed carefully. Cotton wool was used to plug the test tubes, which were then placed on the bench overnight. The mixture was then cooked in a water bath at 100°C for 20 minutes on the second day, and then allowed to cool. The digested blood samples were transferred to a measuring cylinder and filled with distilled water to a volume of 25 ml. Lead residue was determined by using Perkin-Elmer 2380 Atomic absorption spectrophotometer.

Investigation of mRNA expression of Hepcidin gene

This stage was completed at Benha University's Central Laboratory, Faculty of Veterinary Medicine. The following primer sets were used to dissect liver samples from all rat groups (30). Hepcidin, sense (5'-GAAGGCAAGATGGCACTAAGCA-3') and anti-sense (5'-TCTCGTCTGTTGCCGGAGATAG-3'), and actin as a housekeepin gene, sense (5'-AGAAGAGCTATGAGCTGCCTGACGCG-3') and anti-sense (5'-CTTCTGCATCCTGTCAGCGATGC-3').

The Blood Smear (Field stain)

Blood smears are used to look at single-cell spread in blood components (31).

Histopathological examination

Specimens were taken immediately from liver and kidneys of all groups, fixed in 10% buffered neutral formalin for 24 hours. After proper fixation, the specimens were washed in running tape water, dehydrated in different grades of ethyl alcohol, cleared in xylol and embedded in paraffin, then blocked and sectioned as 5 mm thickness. Then stained by hematoxylin and eosin and examined microscopically (32). Pathological alterations were examined using an Olympus light microscope, femur bones were collected, decalcified, fixed and samples were processed (33). All pathological markers were measured using a standard semi quantitative scoring approach to compare the severity of lesion severity between groups. The following is a five-point ordinal scale: (0) no

changes, (1) mild 25 percent tissue damage, (2) moderate 25 percent: 50 percent tissue damage, (3) severe 50 percent: 75 percent tissue damage, and (4) extensive severe >75 percent tissue damage (34).

Statistical analysis

The data was analyzed using SPSS 15.0 statistical software and provided as mean SD (SPSS Inc., Chicago, IL). One analysis of variance (ANOVA) was used for statistical analysis of the current data.

Results

Complete blood count

The mean and standard deviation values of complete blood count of the different experimental groups after 2, 4 and 8 weeks were depicted in Table 1, 2 and 3, respectively. After 2 weeks from the start of the experiment, all measured hematological indices (Hb, PCV, MCV, MCH and MCHC) remained unchanged significantly in both pectin and lead acetate treated groups compared to the control (Table 2). However, after 4 weeks from the start of the experiment, HB, RBCs, PCV, MCH, MCHC values were decreased significantly in lead acetated treated group compared to control (Table 3). These values remained unchanged significantly in pectin treated rats compared to control (Table 3). After 8 weeks from the start of the experiment, all hematological indices were decreased significantly in lead acetate rats (group 3A) compared to control (Table 4). In addition, basophilic stippling cell noticed in this compared to control (Table 4). Co-treatment of rats with lead acetate and pectin recovered all measured hematological indices into normal control values except for MCV and MCHC that remained lower than that of control values (Table 4). Furthermore, basophilic stippling cell was disappeared in rats co-treated with lead acetate and pectin compared to control (Table 4).

Group 1: contained 10 rats that kept as control group. Group 2: contained 10 rats that received pectin at dose of 100 mg/kg BW during experimental period (8 weeks). Group 3: contained 20 rats that received 400mg/kg BW of lead acetate daily for 4 weeks then divided into two subgroups (3A and 3B). Subgroup 3A: contained 10 rats that still receive lead acetate in the same dosage. Subgroup B: contained 10 rats that co-treated with lead acetate and pectin daily for another 4 weeks.

Table 2: effect of lead administration on blood indices in different experimental groups after 2 weeks from the start of the experiment

Parameters	Groups		
	Group 1	Group 2	Group 3
Hb (mg/dl)	14.18±0.52^{a}	12.15±2.41^{a}	12.30±3.70^{a}
RBCs (×10^{6} /µml)	6.71±0.20^{a}	6.32±1.30^{a}	6.42±1.15^{a}
Pcv (%)	36.60±2.35^{a}	37.40±2.24^{a}	39.09±7.54^{a}
MCV (fl/cell)	60.5±1.15^{a}	62.1±2.05^{a}	60.62±2.04^{a}
MCH (pg/cell)	20.43±0.38^{ab}	21.34±2.24^{a}	16.09±4.41^{a}
MCHC (g/dl)	33.90±1.22^{b}	32.80±1.18^{a}	34.77±1.50^{a}

The values represent Mean ± SD. Means within the same row followed by different letters are significantly different (P ≤ 0.05).

Table 3: effect of lead administration on blood indices in different experimental groups after 4 weeks from the start of the experiment.

Parameters	Groups		
	Group 1	Group 2	Group 3
Hb (mg/dl)	14.03±0.30^{a}	13.07±0.51^{a}	9.64±0.07^{b}
RBCs (×10^{6} /µml)	6.83±0.06^{a}	6.99±0.12^{a}	5.12±.0.08^{b}
PCV (%)	34.66±2.52^{a}	33.87±2.49^{a}	26.60±0.2^{b}
MCV (fl/cell)	53.71±1.48^{a}	52.69±1.60^{a}	45.94±2.49^{b}
MCH (pg/cell)	20.97±0.44^{a}	19.88±1.50^{a}	16.01±0.71^{b}
MCHC (g/dl)	38.28±0.37^{a}	36.40±2.40^{a}	31.89±0.49^{b}

The values represent Mean ± SD. Means within the same row followed by different letters are significantly different (P ≤ 0.05).

Table 4: Effect of lead acetate on blood indices in different experimental groups after 8 weeks from the start of the experiment

Parameters	Groups			
	Group 1	Group 2	Group 3	
			3A	3B
Hb (mg/dl)	14 ±0.95[a]	13.45 ±1.67[a]	9.01±0.11[c]	13.3± 0.55[a]
RBCs (×106/µml)	6.00± 0.6[a]	5.88± 0.68[a]	4.50± 0.13[b]	6.22± 0.34[ab]
PCV (%)	35.63± 2.41[a]	32.99± 2.37[a]	28.29 ±0.77[c]	32.36 ±2.43[b]
MCV (fl/cell)	61.48± 1.20[a]	57.88± 1.29[a]	52.13± 0.27[b]	52.08±0.98[b]
MCH (pg/cell)	21.13± 0.4[a]	22.15± 0.51[a]	18.96±0.39[b]	21.26±0.35[a]
MCHC (g/dl)	35.89±1.19[a]	37.99±1.21[a]	31.68±0.51[b]	31.23±1.45[b]
Basophilic Stippling cell	-	-	+	-

The values represent Mean ± SD. Means within the same row followed by different letters are significantly different (P ≤ 0.05).

Table 5: Effect of lead acetate on liver and kidney function tests and iron profile in different experimental groups

Parameters	Groups			
	Group 1	Group 2	Group 3	
			group A	group B
AST (U/ml)	30.10± 3.18[c]	32.21± 2.87[c]	145.62± 4.10[a]	103.7± 1.53[b]
ALT (U/ml)	29.8 ±1.71[c]	31.66 ±2.01[c]	59.33± 0.88[a]	35.91± 3.00[b]
Urea (mg/dl)	25.98± 1.96[c]	27.79± 1.10[c]	131.7± 2.94[a]	42.30± 0.36[b]
Creatinine (mg/dl)	0.68± 0.02[c]	0.64± 0.05[c]	2.9±0.34[a]	0.83± 0.02[b]
Ferritin (ng/dl)	0.7±0.057[a]	0.81±0.07[a]	0.47±0.028[b]	0.70±0.054[a]
Iron (µg/dl)	2.31±0.089[a]	2.42±0.06[a]	1.29±0.10[b]	2.25±0.07[a]
TIBC (mcg/dl)	6.01±0.51[b]	6.06±0.49[b]	8.53±0.24[a]	6.87±0.53[b]

The values represent Mean ± SD. Means within the same row followed by different letters are significantly different (P ≤ 0.05).

Table 6: Effect of lead acetate on oxidative markers, cytokines and lead in different experimental groups

Parameters	Group 1	Group 2	Group 3	
			3A	3B
TAC (µmol/L)	2.45± 0.22[a]	2.51± 0.30[a]	0.99± 0.10[c]	1.93± 0.10[b]
GSH (mg/g)	56.18 ±3.59[a]	55.22±3.60[a]	33.98±2.14[c]	41.45±1.73[b]
NO (µmol/L)	19.06±2.25[c]	20.10±2.40[c]	42.24±1.57[a]	30.11±1.05b[c]
TNF-α (pg/ml)	19.85±5.59[c]	21.99±5.64[c]	59.84 ±4.59[a]	47.45±4.07[b]
IL_6 (pg/ml)	9.87±0.12[c]	9.67±0.24[c]	45.72±1.67[a]	19.64±1.27[b]
Serum lead (mg/dl)	0.95±0.06[a]	0.98±0.07[a]	11.65±0.63[c]	5.95±1.54[b]

The values represent Mean ± SD. Means within the same row followed by different letters are significantly different (P ≤ 0.05). TAC (total antioxidant capacity), GSH (reduced glutathione), NO (nitric oxide).

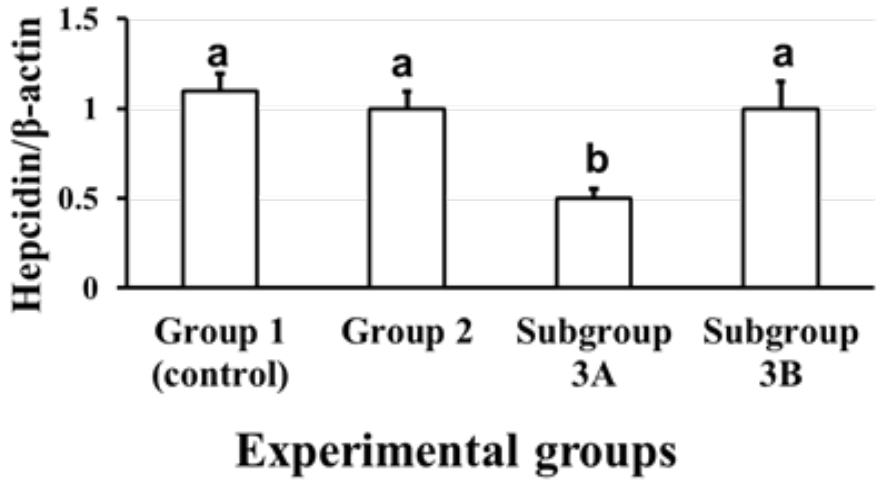

Figure 1: Effect of lead acetate on liver hepcidin mRNA expression level and ameliorative effect of Pectin in male albino rats

Table 7: The score of histopathological lesions in different experimental groups

Lesion score	Group 1	Group 2	Group 3	
			3A	3B
	Liver			
Congestion of hepatic blood vessels	0	0	4	1
Activation of Vonkupfer cell	0	0	3	0
Perivascular Leukocytic infiltration	0	0	3	0
Degenerative changes	0	0	4	1
Necrosis of hepatic cells	0	0	3	0
Nuclear changes	0	0	3	0
	Kidney			
Congestion of renal blood vessels	0	0	3	1
Degeneration of blood vessels wall	0	0	2	0
Perivascular edema	0	0	3	0
Tubular epithelial degeneration and necrosis	0	0	4	1
Hyaline and cellular casts	0	0	2	0
Interstitial leukocytic infiltration	0	0	3	0
necrosis of glomerular tuft	0	0	2	0
	Bone marrow			
Reduction in erythropoiesis	0	0	3	1
Degeneration of myeloid	0	0	2	0

Liver and kidney function tests and iron profile

Activities of ALT and AST and concentrations of urea, creatinine and total iron binding capacity (TIBC) were increased significantly in lead acetate intoxicated group (subgroup 3A) compared to control (Table 5). However, concentrations of serum ferritin and iron, were decreased significantly in lead acetate intoxicated rats (subgroup 3A) compared to control (Table 5). These parameters were improved in rats co-treated with lead acetate and pectin than that of lead acetate treated rats but the normal control values have not been achieved for ALT, AST, urea and creatinine (Table 5).

Oxidative stress biomarkers, cytokines and lead concentrations

The concentrations of NO, TNF-α, IL-6 and lead concentrations were increased significantly in lead acetate intoxicated group (subgroup 3A) compared

to control (Table 6). However, concentrations of serum TAC and GSH were decreased significantly in lead acetate intoxicated rats (subgroup 3A) compared to control (Table 6). These parameters were improved in rats co-treated with lead acetate and pectin than that of lead acetate treated rats but the normal control values have not been achieved (Table 6).

mRNA gene expression

The hepcidin mRNA gene expression of different experimental groups was illustrated in Figure 1. The expression of hepcidin gene in rats fed pectin alone remained unchanged significantly compared to the control (Fig. 1). The expression of hepcidin gene in liver tissue were decreased significantly in lead acetate intoxicated rats (subgroup 3A) compared to control (Fig. 1). Co-treatment of rats with lead acetate and pectin (subgroup B3) up-regulated the expression of this gene to normal control value (Fig. 1).

Histopathological examination

The score of lesions of histopathological examination were seen in the liver, kidneys, and bone marrow of rats in different experimental groups as shown in Table 7. The histopathoogical picture of rats tissues that received pectin only (group 2) were not showed in the current study because it looks like the control group (group 1) as illustrated in Table 7.

The histological examination of the liver in subgroup 3A showed that there were congestion of the hepatic blood arteries and blood sinusoids, as well as portal distension and leukocytic cellular infiltration, primarily lymphocytes and macrophages (figure 2A). Hepatocytes also showed significant degeneration in the form of diffuse hydropic degeneration (figure 2B) with diffuse hemorrhage in the hepatic parenchyma, as well as multifocal patches of coagulative necrosis with pyknotic nucleus. Furthermore, diffuse regions of lytic necrosis in the hepatic parenchyma were detected, that consisted of necrotic debris mixed with erythrocytes and leukocytes (figure 2C&D). The hepatic tissue collected from rats in subgroup 3B showed an improvement in the hepatocellular architecture when compared with rats in subgroup 3A. In comparison to the control, the liver tissue returned to its normal histological structure. The majority of the hepatic parenchyma had recovered, and only minor hepatocyte vacuolar degeneration (figure 2E) was observed, while the portal area appeared normal. The microscopic analysis of hepatic tissue from control and pectin treated groups showed normal histological structure and showed in the figure.

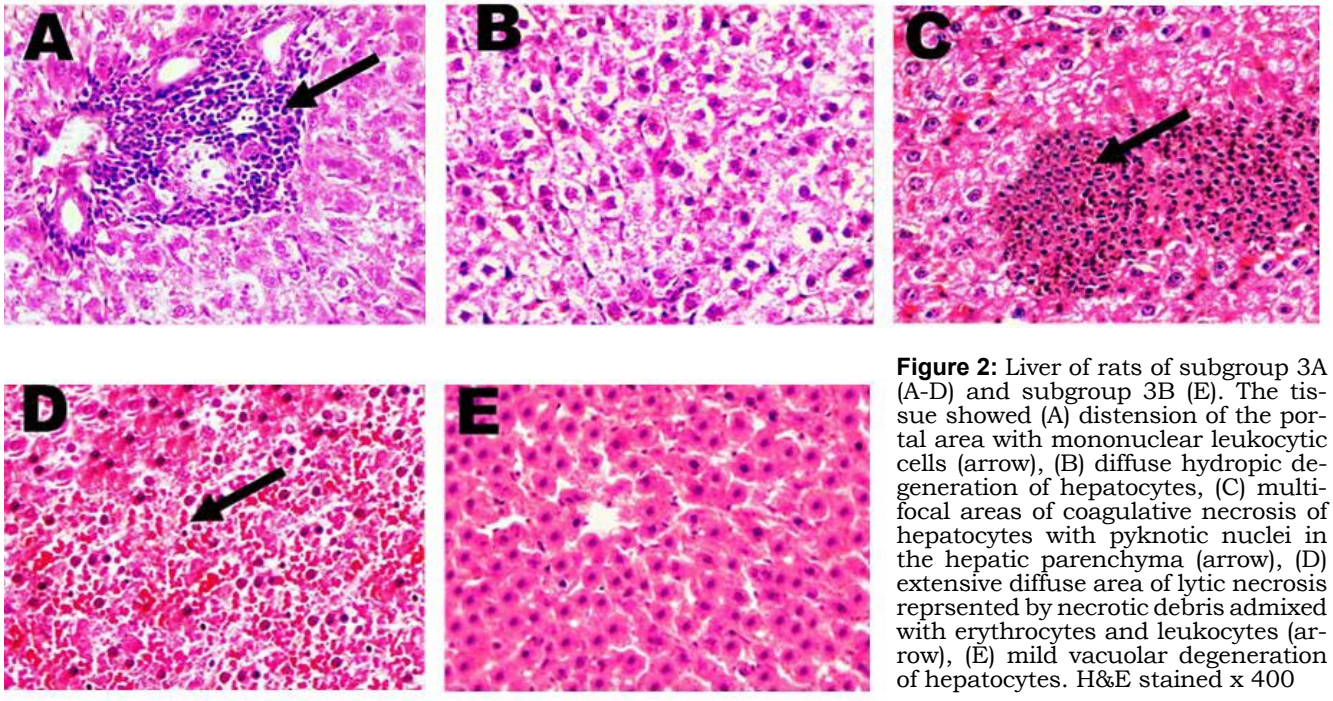

Figure 2: Liver of rats of subgroup 3A (A-D) and subgroup 3B (E). The tissue showed (A) distension of the portal area with mononuclear leukocytic cells (arrow), (B) diffuse hydropic degeneration of hepatocytes, (C) multifocal areas of coagulative necrosis of hepatocytes with pyknotic nuclei in the hepatic parenchyma (arrow), (D) extensive diffuse area of lytic necrosis reprsented by necrotic debris admixed with erythrocytes and leukocytes (arrow), (E) mild vacuolar degeneration of hepatocytes. H&E stained x 400

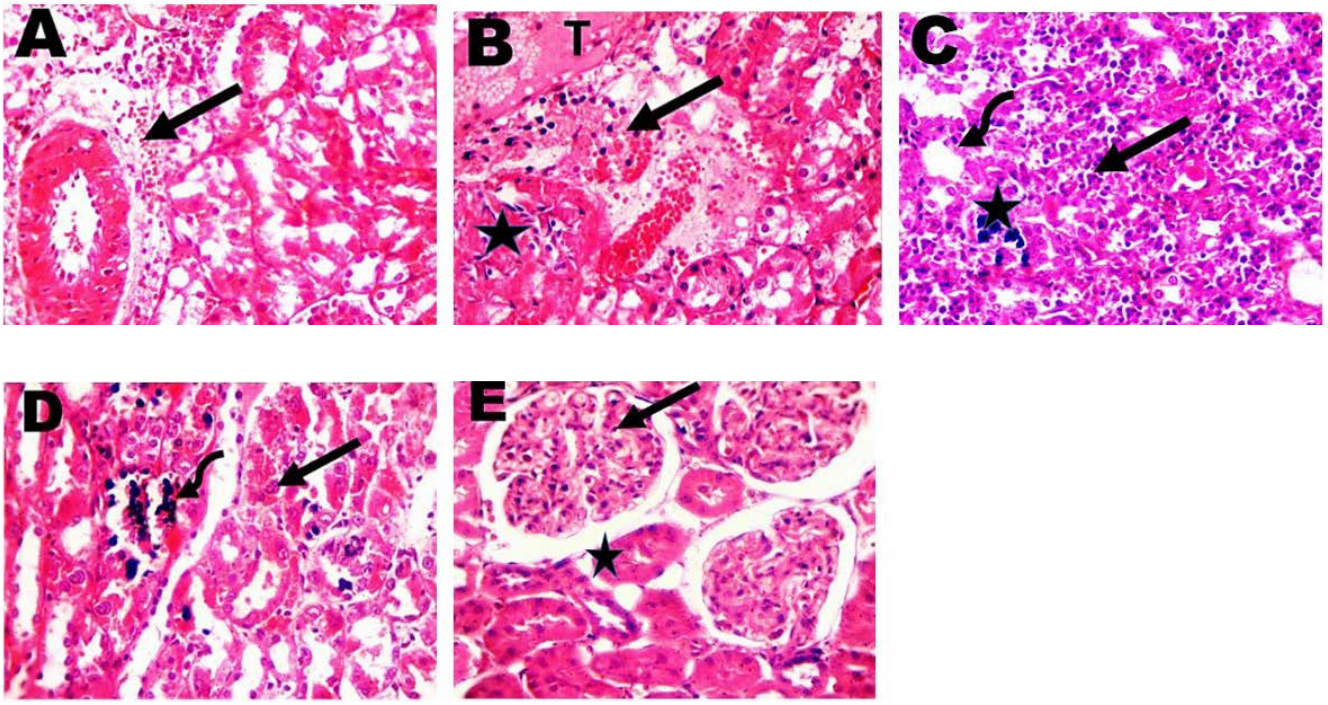

Figure 3: kidney of rats for subgroup 3A(A-D) and subgroup B (E). tissue showed (A) perivascular edema admixed with erythrocytes (arrow) with vacuolar degeneration of the lining epithelium of some renal tubules and its necrosis with pyknotic nuclei in other tubules, (B) necrosis of the glomerular tuft (asterisk) and with thrombosis of the renal blood vessels (T) with extensive focal area of lytic necrosis represented by necrotic debris admixed with erythrocytes and leukocytes (arrow), (C) necrosis of the lining epithelium of the con-voluted tubules (zigzag arrow), inter tubular mononuclear leukocytic cellular infiltrations (arrow) with precip-itation of lead pigment renal tubules (asterisk), (D) precipitation of lead pigment in the renal tubules of renal medulla (zigzag arrow) with the presence of intra-nuclear eosinophilic inclusion bodies (arrow), (E) mild vacuolation of the endothelial cell lining of glomerular tuf with cloudy swelling of the lining epithelium of some renal tubules. H&E stain x 400

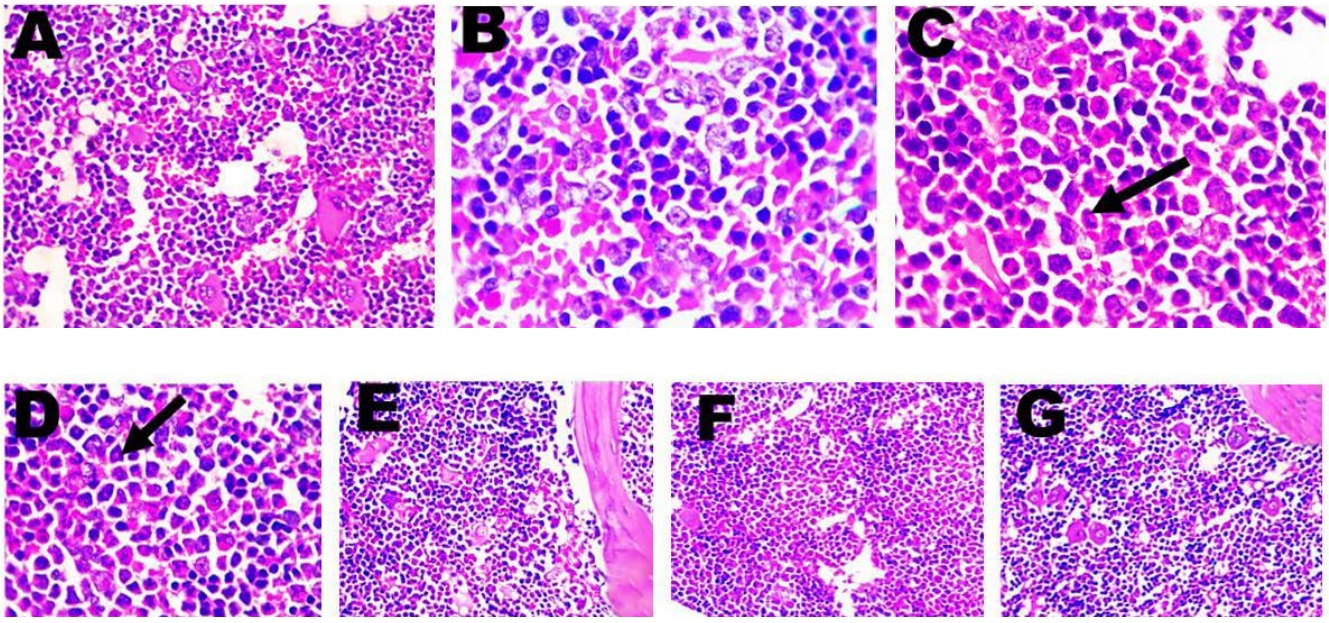

Figure 4: Bone marrow of rats for control (A-B), subgroup 3A (C-E) and subgroup 3B (F-G), showing (A-B) nor-mal bone marrow (A, x400, B, x1000), (C) degeneration and apoptosis of myeloid cells (arrow, x1000), (D) intra-nuclear eosinophilic inclusion bodies (arrow, x1000), (E) degeneration of megakaryocytes (x1000), (F) hyperplasia of megakaryocytes (x1000), (G) restoring of normal histological structure of bone marrow (H&E-stained x1000)

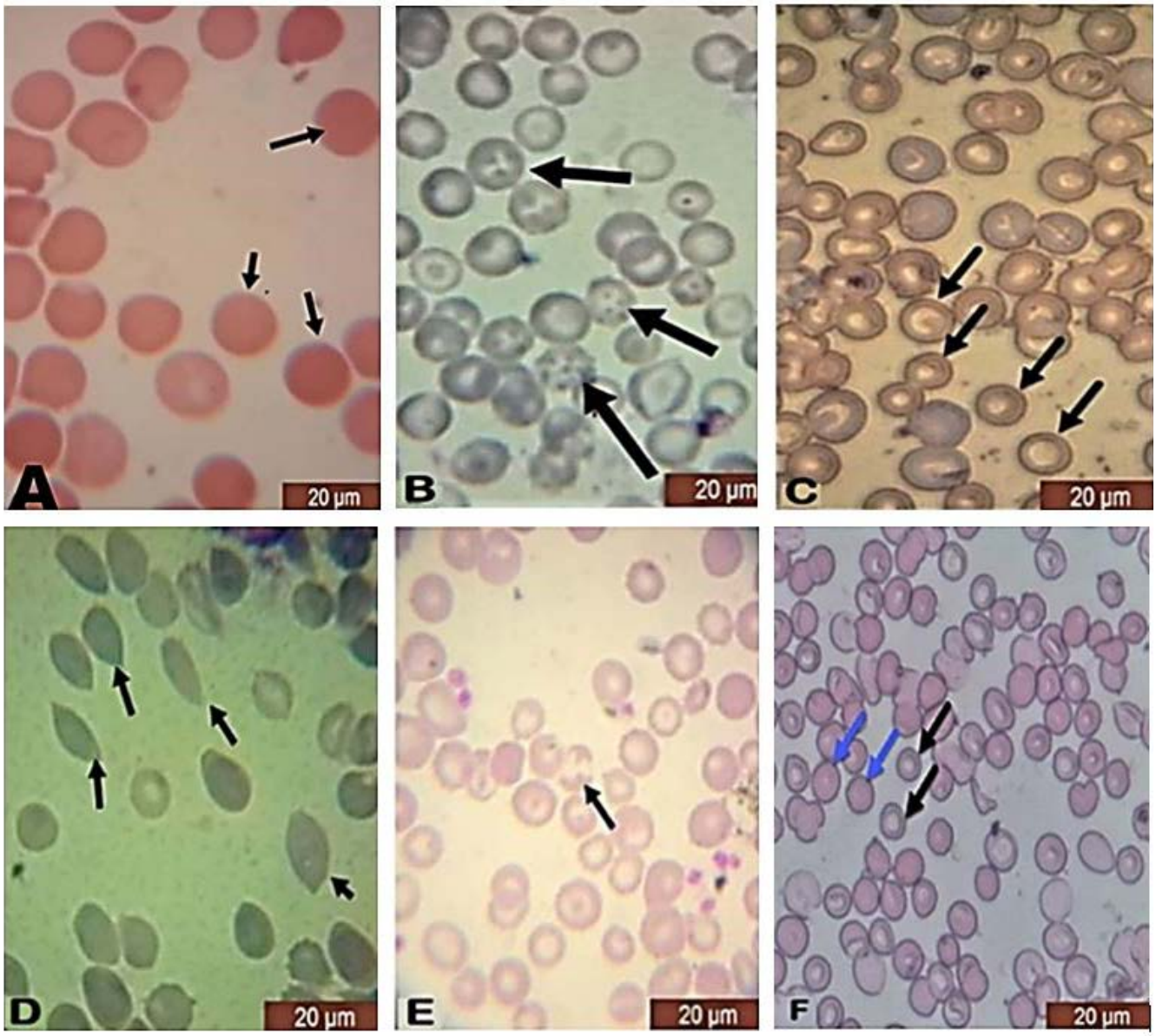

Figure 5: Blood smear of rats. (A) normal RBCs of control group, (B-E) RBCs of subgroup 3A (B) basophilic gran-ules in RBCs (C) hypo chromatic RBCs, (D) tear drops RBCs (E) hemolysis of RBCs. (F) RBCs of group B blue arrow nor-mal RBCs and black arrow hypo chromatic RBCs

The renal blood vessels, inter-tubular and glomerular blood capillaries, and perivascular edema mixed with erythrocytes were all congested in the kidneys retrieved from subgroup 3A (figure 3A). Thrombosis of the renal blood vessels with vacuolation of the glomerular endothelial cells, as well as necrosis of the glomerular tuft in some cases in association with focal area of lytic necrosis characterized by complete absence of renal tissue and replaced by eosinophilic debris with erythrocytes and few leukocytes (figure 3B) were also detected. In addition, extensive degenerative changes in the lining epithelium of the renal tubules were observed in the renal cortex, including vacuolation, hydropic degeneration, desquamation and necrosis with pyknotic nuclei in association with eosinophilic hyaline casts in the lumen of some renal tubules, mononuclear leukocytic cellular infiltrations in interstitial tissue with precipitation of lead pigment In most deteriorated epithelial cells, clumps of amorphous blue staining lead pigment were precipitated in varying quantities in the cytoplasm of the degenerated tubules of the renal medulla in conjunction with intra-nuclear eosinophilic inclusions (figure 3D). While in subgroup 3B showed improvement in the degenerative changes in the kidneys caused by lead acetate. A microscopical examination of

the kidney from subgroup 3B demonstrated a significant improvement in renal tissue histology when compared to subgroup 3A. There was mild congestion of the renal blood arteries and glomerular blood capillaries with normal histological structure of the glomeruli. Meanwhile, mild vacuolation of the endothelial cell lining of the glomerular tuft was observed in some cases (Figure 3E), along with mild degenerative changes in the lining epithelial cell of the renal tubules in the form of cloudy swelling, while control and pectin treated group's revealed normal renal histological structure.

Compared to the control group bone marrow (Figure 4a-b), a marked reduction in erythropoiesis was demonstrated in the bone marrow of lead intoxicated rats (subgroup 3A) as well as degeneration of myeloid cells, especially megakaryocytes, apoptosis of myeloid cells with the presence of intranuclear eosinophilic inclusion bodies was detected (Figure 4C-E). On the other side, a reduction in the pathological alterations induced by lead toxicity was observed in the bone marrow of rats in subgroup B as an increase in cell density affecting erythroid and myeloid cells with megakaryocytic hyperplasia in proportion to the other cells types (Figure 4F-G).

The Blood Smear (Field stain)

Blood smears were used to look for abnormal red blood cells as basophilic granulation, hypo chromatic, tear drops and hemolysis of RBCs Figure 5(B-E) which considered as important marker for lead toxicity, this may explain that lead causes anaemia and there were basophilic stippling cell noticed in subgroup 3A compared to other experimental groups.

Discussion

Lead is one of the most hazardous heavy metals on the human and animals. It is one of the most serious environmental pollutants. It used by humankind for many years due to its wide range of applications. Lead enters the body through a variety of routes, including the air, food, dust, soil, and water (35). Adult Wister rats were exposed to lead, had toxic effects in their blood, liver, and kidneys.

Oxidative stress is a primary mechanism of metal toxicity, and it was identified as a significant factor in our investigation when we discovered an altered redox state in treated rats' tissues as well as hematological problems (5). The activity of Aminolevulinic acid dehydratase (ALAD) is severely inhibited by lead, which disrupts haeme anabolism (36). The significant decrease of hematological indices (RBCs, Hb, MCH and MCHC) in lead acetate intoxicated rats indicated a state of anemia. This finding may be attributed to chelating properties of lead acetate (37). Lead can bind to essential minerals in the body, producing a variety of physiological problems in addition to affecting protein production and inhibiting hemoglobin formation (37). The protective effect of pectin as demonstrated in the current study was consistent with previous findings (18) which recorded the pectin's ability to chelate metals in the digestive system and inhibit absorption while aiding their removal in the faces (14). RBCs, Hb, PCV %, MCV, MCH, and MCHC were all lower in microcytic hypochromic anemia (39). In the current study, subgroup 3A showed that lead toxicity to rats induced microcytic hypochromic anemia, as it decreased RBCs, Hb, PCV%, MCV, MCH and MCHC, which in accordance with the results reported previously (40). Lead inhibits several enzymes that are important for haeme synthesis (41), and lead suppresses enzymatic activities such amionlevulinic acid dehydratase (ALAD), and ferochelatase, which are all important for haeme production, this suppression leads to a problem with iron metabolism (18). However, on the other hand, subgroup 3B showed an improvement in blood indices (RBCs, Hb, PCV%, MCV, MCH, and MCHC) when compared to subgroup 3A which in the same line of previous work (38) showed that date pectin extract was effective when taken orally for one month boosted RBC, Hb, MCV and MCH levels significantly ($P \leq 0.05$). previous work (42) demonstrated that low-esterified pectin quickly forms complexes with divalent metals, including ions of hazardous elements (mercury, lead, and cadmium), hence, reduced the cytotoxic effects of heavy metals. Histopathological examination of bone marrow in subgroup 3A (Figure 4c, e) explained that a marked reduction in erythropoiesis as well as degeneration of myeloid cells, especially megakaryocytes and apoptosis of myeloid cells were observed. While in subgroup 3B (Figure 4f, g)

hyperplasia of megakaryocytes and restoring of normal histological structure of bone marrow was observed and this explained the anemic picture improvement that appeared in blood indices of rats co-treated with lead acetate and pectin. Lead toxicity in subgroup 3A causing abnormal red blood cells which clear in blood smear (field stain) shown in figure 5 B1-B4) development of basophilic granules, hypo chromatic, tear drops and heamolyzied RBCs, which are characteristics of anemia caused by lead poisoning (43, 44), as previously noted (45). While in subgroup 3B, figure (5C) showed, only hypo chromatic RBCs due to protective effect of pectin. Our investigations (Figure 1) revealed significant ($P \leq 0.05$) decrease in hepcidin gene expression of subgroup 3A in comparison by control and subgroup 3B. This finding is parallel to previous work (9, 10) reported that Hepcidin gene expression is reduced following experimentally induced anemia and hypoxia. This could explains the increased iron release from reticuloendothelial cells and Hepcidin participation in anemic conditions is revealed by increased iron absorption in these settings and iron transfer from endosomes to the cytoplasm has also been found to be inhibited by lead. Subgroup 3B showed significant elevation in hepcidin expression gene ($P \leq 0.05$) which attributed to Pectin's ability that chelate metals in the digestive system and inhibit absorption while aiding their removal in the faces (14). In present study, subgroup 3A showed that, serum ferritin (iron store) and iron levels decreased significantly, in despite of increment of TIBC levels compared to the control. This result is in agreement with previous work (46) revealed that lead poisoning can cause anemia by interfering with haeme production, resulting in iron shortage. More recently (4), rats exposed to lead were found to have lower serum iron and transferrin saturation levels. The significant increase of TIBC could be related to higher production of transferrin by the liver in an attempt to make the most of the iron that is available (47). More over subgroup 3B showed an increasing of serum iron and ferritin and decreased TIBC as pectin rich in galacturonic acid (GalA) effectively chelate heavy metals (13, 48) suggesting that iron (Fe) bound to pectin is utilized by rats and enhancing the final Hb content. The current study demonstrated that liver functions in lead acetate intoxicate group had significantly higher AST and ALT activities than that of the control. These differences could be due to the toxic effect of lead acetate, which causes those enzymes to be released by increasing hepatocyte permeability or damaging the cell membrane of hepatocytes. In addition, lead toxicity produced an increase in cellular basal metabolic rate, irritability, and destructive alteration of liver cells (5, 49). As well as the creation of free radicals by lead caused harmful effect on hepatocytes, which reinforced by our histopathological picture showing in fig (5A-D) in subgroup 3A. This figure showed diffuse hydropic degeneration of hepatocytes in the hepatic parenchyma, multifocal regions of coagulative necrosis of hepatocytes with pyknotic nuclei and extensive diffuse regions of lytic necrosis with mild vacuolar degeneration of hepatocytes. The same picture showed mild amelioration of histpathological alternation in subgroup B (fig5 E), which showed mild vacuolar degeneration of hepatocytes, as majority of the hepatic parenchyma appeared to be improved may be due to treatment with Low-esterified pectin rapidly forms complexes with divalent metals as lead which are poisonous decreasing heavy metal cytotoxicity (42, 50). Previous study (38) found that ALAD activities were boosted by pectin treatment and decreased lipid peroxidation product in rat, as well as a significant increase in erythrocyte-SOD (Super oxide dismutase) and GSH activities, indicating that pectin protects body cells from oxidative radicals caused by lead. The significant increase of urea and creatinine lead acetate treated group compared to the control agrees with previous work (6) which recorded oral dose of lead acetate caused a significant rise in blood urea and serum creatinine. These results confirmed histopathologically (fig6 A-D), showed perivascular edema admixed with erythrocytes with necrosis of the glomerular tuft and thrombosis of the renal blood vessels with severe localized lytic necrosis, necrosis of the convoluted tubule lining epithelium, and moderate vacuolation of the glomerular tuft endothelial cell lining with cloudy swelling of the lining epithelium of some renal tubules. Slight improvement was observed in subgroup 3B as reflected on significant decrease of these parameters compared to that of subgroup 3A. These findings have been confirmed by hispathological picture (fig 6 E), that revealed improvement in renal tissue histology. This improvement was in the forms of mild vacuolation of the endothelial cell lining of the glomerular tuft

with mild degenerative changes in the lining epithelial cell of the renal tubules epithelium of some renal tubules, mild congestion of the renal blood vessels and glomerular blood capillaries with normal histological structure of the glomeruli. These findings were hand in hand with the improvement of functions the liver and kidney recorded earlier (50) with aresinic toxicity and co-treatment with pectin. This may be due to pectin hastened the elimination of arsenic in faces by lowering intestinal absorption, preventing buildup, and reducing arsenic toxicity. The exposure to lead acetate in subgroup 3A reduced the GSH activities and increased Nitric Oxide (NO) activity when compared to control. This result is comparable to that of a previous study of lead toxicity (38) caused oxidative stress, depletion of rapid antioxidants, higher production of reactive oxygen and nitrogen species and activation of lipid peroxidation. Thus, increasing oxidative stress induced a decrease in GSH levels, resulting in a decrease in glutathione concentration (3, 7). While in subgroup 3B, there were an improvement, as TAC and GSH were significantly elevated while Nitric Oxide activity was reduced. This finding may attributed to ROS scavenging activity of pectin, which is known to be reliant on pectin structural properties (51, 52). Present study showed that serum TNF-α and IL-6 in subgroup 3A increased significantly compared to the control group. Smilar results of (53) found that exposure to low lead level caused an increase of pro-inflammatory cytokines, such as TNF-α with a corresponding increase in other cytokines, such as IL-10, a T cell cross-regulatory factor, suggesting possible interference of lead in the immunophlogosis system. Lead has been found to enhance TNF- α production in vitro by human peripheral mononuclear cells (54). TNF-α is made primarily by activated macrophages and lymphocytes at the site of inflammation, and it plays a role in local and systemic inflammatory reactions with IL-6 and IL-1. It participates in local and systemic inflammatory reactions. Previous work (55) found that lead boosted total TNF- α cell expression in PBMC (+1ng/mL LPS). Pervious study (56) showed that blood levels of interleukin 6 (IL-6) and tumor necrosis factor (TNF- α) of 56 male workers chronically exposed to lead were significantly higher than that of the control group. In the current study, both TNF-α and IL-6 showed significant reduction in subgroup B compared to the control. This explained previously that commercially available Pectin had a pro-inflammatory effect in the spleen of BALB/c mice, up regulating cytokine release, including IL-17, IFN-, and (TNF- α), independent of Gal-3 inhibition (57). Moreover, pectin had a similar reducing effect on (TNF- α) and IL-10 secretion resulting in a higher survival rate in endotoxin-shocked mice (58). Citrus pectin has also been proven to inhibit the production of interleukin-6 (IL-6) and lowered the inflammatory cytokine gene expression (59).

Conclusion

Present study on lead toxicity on rats demonstrated a hazards effect on Hepcidin expression gene, serum iron profile, blood indices, and liver and kidney functions, oxidative and pro inflammatory effects. So to manage lead toxicity it is necessary to use a specific chelating agent and in the same time. Pectin may be regarded nutritional items that could be utilized to reduce lead intestine absorption, minimize lead buildup, and ameliorate lead poisoning because they are both selective and effective in interacting with lead. We concluded that daily pectin ingestion is recommended in highly polluted areas with lead.

Acknowledgement

This work was supported through the Annual Funding track by the Deanship of Scientific Research, Vice Presidency for Graduate Studies and Scientific Research, King Faisal University, Saudi Arabia (Project No. AN000478; GRANTI656).

References

1. Mañay N, Cousillas A, Alvarez CTH. Lead contamination in Uruguay: The “La Teja” neighborhood case. Rev Environ Contamtoxicol 2008; 195: 93–115.

2. Klauder D, Petering HG. Anemia of lead intoxication: a role of copper. J Nutr 1977; 107: 1779–85.

3. Rehman K, Fatima F, Waheed I. Prevalence of exposure of heavy metals and their impact on health consequences. J Cell Biochem 2018; 119: 157–84.

4. Moshtaghie M, Malekpouri P, Dinko MR, Moshtaghie AA. Changes in serum parameters as-

sociated with iron metabolism in male rat exposed to lead. J Physiol Biochem 2013; 69: 297–304.

5. Andjelkovic M, Buha Djordjevic A, Antonijevic E, et al. Toxic effect of acute cadmium and lead exposure in rat blood, liver, and kidney. Int J Environ Res Public Health 2019; 16: e274. doi: 10.3390/ijerph16020274

6. Elayat W, Bakheetf MS. Effects of chronic lead toxicity on liver and kidney functions. J Med Lab Sci 2010; 1: 29–36.

7. Zhushan F, Shuhua X. The effects of heavy metals on human metabolism. Toxicol Mech Methods 2020; 30: 167–76.

8. Qian ZM, Xiao DS, Wang Q, et al. Inhibitory mechanism of lead on transferrin-bound iron uptake by rabbit reticulocytes: a fractal analysis. Mol Cell Biochem 1997; 173: 89–94.

9. Theurl I, Aigner E, Theurl M, et al. Regulation of iron homeostasis in anemia of chronic disease and iron deficiency anemia: diagnostic and therapeutic implications. Blood 2009; 113: 5277–86.

10. Theurl I, Schroll A, Nairz M, et al. Pathways for the regulation of hepcidin expression in anemia of chronic disease and iron deficiency anemia in vivo. Haematologica 2011; 96(12): 1761–9.

11. Muckenthaler MU. Fine tuning of hepcidin expression by positive and negative regulators. Cell Metab 2008; 8: 1–3.

12. Drochner W, Kerler A, Zacharias B. Pectin in pig nutrition, a comparative review. J Anim Physiol Anim Nutr (Berl) 2004; 88: 367–80.

13. Vakkalanka DR, MS Oic, Chau HK, et al. Pectic oligosaccharide structure-function relationships: prebiotics, inhibitors of *Escherichia coli* O157:H7 adhesion and reduction of Shiga toxin cytotoxicity in HT29 cells. Food Chem 2017; 227: 245–54.

14. Eliaz I, Hotchkiss AT, Fishman ML, Rode D. The effect of modified citrus pectin on urinary excretion of toxic elements. Phytother Res 2006; 20: 859–4.

15. Paskins H, Tanaka Y, Skoryna S, Moore W, Stara J. The binding of lead by a pectic polyelectrolyte. Environ Res 1977; 14: 128–40.

16. Ostapenko VA, Teplyakov AI, Chegerova TI. Efficiency of apple pectin for prophylaxis of lead incorporation in workers. Med Truda I Promyshlennaya Ekol 2001; 5: 44–7.

17. Siu W, Ko E, Lee H, et al. A food supplement with lead chelating effect: a preliminary study. J Heavy Met Toxic Dis 2017; 2: 16. doi: 10.21767/2473-6457/1000016

18. Okediran BS, Biobaku KT, Olaifa1 FH, Atata AJ. Haematological and antioxidant enzyme response to lead toxicity in male wistar rats. Ceylon J Sci 2017; 46: 31–7.

19. Reitman S, Frankel SA. Colorimetric method for the determination of serum glutamic oxalacetic and glutamic pyruvic transaminases. Am J Clin Pathol 1975; 28: 56–63.

20. Patton CJ, Crouch SR. Spectrophotometric and kinetics investigation of the berthelot reaction for the determination of ammonia. Anal Chem 1977; 49: 464–9.

21. Jaffé MUDN. Welchen pikrinsäure in normalem harn erzeugt und über eine neue reaction des kreatinins. Biol Chem 1986; 10: 391–400.

22. Ceriotti F, Ceriotti G. Improved direct specific determination of serum iron and total iron-binding capacity. Clin Chem 1980; 26: 327–31.

23. Linpisarn S, Kricka LJ, Kennedy JH, Whitehead TP. Sensitive sandwich enzyme immunoassay for serum ferritin on microtitre plates. Ann Clin Biochem 1981; 18: 48–53.

24. Fischl J, Cohen SA. Simple colorimetric method for the determination of total iron-binding-capacity of serum. Clin Chim Acta 1962; 7: 121–3.

25. Erel O. A novel automated method to measure total antioxidant response against potent free radical reactions. Clin Biochem 2004; 37(2) :112–9.

26. Moron MS, Depierre BM. Levels of glutathione, glutathione reductase and glutathione-s-transferase activities in rat lung and liver. Biochem Biophys Acta 1979; 582: 67–72.

27. Montgomery H, Doymock J. Colorimetric determination of nitric oxide. Analyst 1961; 86: 414–6.

28. Chen W, Jin W, Cook M, Weiner LH, Wahl MS. Oral delivery of group a streptococcal cell walls augments circulating TGF-beta and suppresses streptococcal cell wall arthritis. J Immunol 1998; 161: 6297–304.

29. Hegazy AM, Fakhreldin AR, Nasr SN. Monitoring of carcinogenic environmental pollutants in women's breast milk. Biomed Pharmacol J 2020; 13(1): 119–25.

30. Gasparino E, Del Vesco AP, Voltolini DM, et al. The effect of heat stress on GHR, IGF-I, ANT, UCP and Coxiii mRNA expression in the liver and muscle of high and low feed efficiency female quail. Br Poult Sci 2014; 55: 466–73.

31. Ragan P, Turner T. Working to prevent lead poisoning in children: getting the lead out. JAAPA 2009; 22: 40–5.

32. Suvarna SK, Layton C, Bancroft JD. 2012. Bancroft's theory and practice of histological techniques. 7th ed. Oxford : Churchill Livingstone, 2012.

33. Luna GL. Manual of histological and special staining techniques of the Armed Forces Institute of Pathology. 3rd ed. New York : McGraw Hill, 1968: 9–34.

34. Hassanen E, Khalaf A, Zaki A, et al. Ameliorative effect of ZnO-NPs against bioaggregation and systemic toxicity of lead oxide in some organs of albino rats. Environ Sci Pollut Res 2021; 28(28): 37940-52.

35. Herman D, Geraldine M, Venkatesh T. Evaluation, diagnosis, and treatment of lead poisoning in a patient with occupational lead exposure: aA case presentation. J Occup Med Toxicol 2007; 2: 7–10.

36. Dorward A, Yagminas A. Activity of erythrocyte δ-aminolevulinic acid dehydratase in the female cynomolgus monkey (*Macaca fascicularis*): kinetic analysis in control and lead-exposed animals. Comp Biochem Physiol Part B Comp Biochem 1994; 108: 241–52.

37. Patrick L. Lead toxicity part II: the role of free radical damage and the use of antioxidants in the pathology and treatment of lead toxicity. Altern Med Rev 2006; 11: 114–27.

38. Nesrine S, Ouldali O, Bekara A, et al. Effect of pectin extract of date (*Phoenix dactylifera* l) on erythrocytes oxidative damage and hematological parameters induced by lead in males rats. J Appl Environ Biol Sci 2016; 6(10): 41–9.

39. Zhang X, Xie P, Li D, Shi Z. Hematological and plasma biochemical responses of crucian carp (*Carassius auratus*) to intraperitoneal injection of extracted microcystins with the possible mechanisms of anemia. Toxicon 2007; 49: 1150–7.

40. El-Bahr SM, Amal ME, Nashwa EG, et al. Biosynthesized iron oxide nanoparticles from *petroselinum crispum* leaf extract mitigate lead-acetate-induced anemia in male albino rats: hematological, biochemical and histopathological features. Toxics 2021; 9(6): e123 . doi: 10.3390/toxics9060123

41. Aly MH, Kim HC, Renner SW, et. al. Hemolytic anemia associated with lead poisoning from shotgun pellets and the response to succimer treatment. Am J Hematol 1993; 44: 280–3.

42. Dalia MEN. Effect of using pectin on lead toxicity. J Am Sci 2010; 6(12): 541–54.

43. Alleman H, Consendey B, Lob M. Lead poisoning by cutaneous drug absorption. Swiss Med Wkly 1986; 116: 888–91.

44. Ouldali O, Meddah M, Slimani M, et al. Beneficial effects of carrot pectin against lead intoxication in waster rats. Int J Green Pharmacy 2011; 5: 126-–31.

45. Noori M, Mohammad H, Zahra H, et al. Effects of chronic lead acetate intoxication on blood indices of male adult rat . DARU J Pharmaceut Sci 2003; 11(4): 147.

46. Rey V, ´Azquez G, Guerrero GA. Characterization of blood cells and hematological parameters in *Cichlasoma dimerus* (Teleostei, Perciformes). Tissue Cell 2007; 39(3): 151–60.

47. Elshemy MAE. Iron oxide nanoparticles versus ferrous sulfate in treatment of iron deficiency anemia in rats. Egypt J Vet Sci 2018; 49: 103–9.

48. Tomihiro M, Akira N, Kiyoshi E. Iron bound to pectin is utilized by rats. Br J Nutr 2011; 106: 73–8.

49. Ibrahim NM, Eweis EA, El-Beltagi H S, Abdel-Mobdy YE. Effect of lead acetate toxicity on experimental male albino rat. Asian Pac J Trop Biomed 2012; 2: 41–6.

50. Fahmy HA, Sayed AEF, Omar TM. Effect of low and high-esterified pectin on arsenic toxification in rats. J Biol Chem Environ Sci 2008: 3: 11–33.

51. Liu SX, Shi L, Xu YY. Optimization of pectin extraction and antioxidant activities from Jerusalem artichoke. Chin J Oceanol Limnol 2016; 34: 372–81.

52. Wang W, Xiaobin M, Peng J. Characterization of pectin from grapefruit peel: a comparison of ultrasound–assisted and conventional heating extractions. Food Hydrocolloids 2016; 61: 730–9.

53. Rrocova Z, Macela A, Kroca M, Hernychova L. The immunomodulatory effect(s) of lead and cadmium on the cells of immune system in vitro. Toxicol In Vitro 2000; 14(1): 33–40.

54. Guo T, Mudzinski S, Lawrence D. The heavy metal lead modulates the expression of both TNF-alpha and TNF-alpha receptors in lipopolysaccharide-activated human peripheral blood mononuclear cells. J Leukoc Biol 1996; 59(6): 932–9.

55. Turner MD, Nedjai B, Hurst T. Pennington DJ. Cytokines and chemokines: at the crossroads of cell signalling and inflammatory disease. Biochim Biophys Acta 2014; 1843(11): 2563–82.

56. Anna MG, Michal D, Aleksandra K, et al. The effect of subacute lead exposure on selected blood inflammatory biomarkers and angiogenetic factors. J Occup Health 2018; 60(5): 369–75.

57. Merheb R, Abdel-Massih RM, Karam MC. Immunomodulatory effect of natural and modified citrus pectin on cytokine levels in the spleen of balb/c mice. Int J Biol Macromol 2019; 121: 1–5. doi: 10.1016/j.ijbiomac.2018.09.189

58. Popov SV, Ovodov YS. Polypotency of the immunomodulatory effect of pectins. Biochemistry 2013; 78: 823–35.

59. Ishisono K, Yabe T, Kitaguchi K. Citrus pectin attenuates endotoxin shock via suppression of toll-like receptor signaling in peyer's patch myeloid cells. J Nutr Biochem 2017; 50: 38–45.

PEKTIN VPLIVA NA IZBOLJŠANJE HEMATOLOŠKIH IN BIOKEMIJSKIH PARAMETROV, HISTOPATOLOGIJE, BIOLOŠKIH OZNAČEVALCEV OKSIDATIVNEGA STRESA, CITOKINOV TER IZRAŽANJE GENA ZA HEPCIDIN PRI S SVINCEM POVZROČENI TOKSIČNOSTI PRI PODGANAH

S. M. El-Bahr, S. Al-Sultan, A. F. Hamouda, S. A. E. Atwa, S. Y. Abo-Kora, A. A. Amin, S. Shousha, S. Alhojaily, A. Alnehas, R. R. Elzogby

Izvleček: Objav o zaščitnem učinku pektina pred toksičnostjo svinca pri podganah ni na voljo. Da bi proučili ta učinek, smo 40 samcev podgan razdelili v 3 skupine. V prvi, kontrolni skupini je bilo 10 podgan. V drugi skupini je bilo 10 podgan, ki so v poskusnem obdobju (8 tednov) prejemale pektin v odmerku 100 mg/kg telesne teže. V tretji skupini je bilo 20 podgan, ki so 4 tedne dnevno prejemale svinčev acetat v odmerku 400 mg/kg telesne teže. Tretja skupina je bila nato razdeljena v dve podskupini (3A in 3B). V podskupini 3A je bilo 10 podgan, ki so še naprej 4 tedne prejemale svinčev acetat v enakem odmerku, v podskupini 3B pa je 10 podgan prejemalo svinčev acetat in pektin. Vzorci krvi so bili odvzeti po 2, 4 in 8 tednih od začetka poskusa. Ob koncu poskusa so bili odvzeti še jetra, ledvice in kostni mozeg. Svinčev acetat je povzročil anemijo šele po štirih tednih, kar se je kazalo v zmanjšanih vrednostih Hb, PCV, MCV, MCH in MCHC. V skupini podgan, ki so prejemale svinčev acetat, so te vrednosti do konca poskusa ostale nizke. Koncentracije serumskega feritina, železa, skupne antioksidativne kapacitete (TAC), reduciranega glutationa (GSH) in izražanje jetrnega gena za hepcidin so se pri podganah, ki so prejemale svinčev acetat, znatno zmanjšale v primerjavi s kontrolo. Aktivnosti ALT in AST ter koncentracije sečnine, kreatinina, dušikovega oksida (NO), TNF-α, IL-6, skupne kapacitete vezave železa (TIBC) in svinca so se v skupini, ki je prejemala svinčev acetat, znatno povečale v primerjavi s kontrolno skupino. Najvidnejše spremembe pri podganah, ki so prejemale svinec, so bile jetrna degeneracija in krvavitve, ledvična nekroza in apoptoza mieloidnih celic. Spremembe, povezane s svinčevim acetatom, so se izboljšale s sočasnim zdravljenjem s pektinom, vendar normalne kontrolne vrednosti niso bile dosežene. Zaključili smo, da je pektin priporočljiv za zaščito pred toksičnostjo svinčevega acetata pri podganah.

Ključne besede: svinčev acetat; toksičnost; pektin; hepcidin; biološki označevalci oksidativnega stresa; histopatologija

Slov Vet Res 2022; 59 (4): 211–17
DOI 10.26873/SVR-1286-2022
UDC 599.742.28:591.2:616-091.5(513.1)

Case Report

PATHOLOGICAL FINDINGS IN AN OLD FEMALE GIANT PANDA – A CASE REPORT

Bangyuan Wu[1,2,3], Juan Wang[3], Tong Cai[3], Chengdong Wang[5], Desheng Li[5], Linhua Deng[5], Xi Peng[4]*

[1]Key Lab of Animal Ecology and Conservation Biology, Institute of Zoology, Chinese Academy of Sci-ences, 1-5 Beichenxi Road, Chaoyang, 100101 Beijing, [2]Key Laboratory of Southwest China Wildlife Re-sources Conservation (Ministry of Education), [3]College of Life Science, China West Normal University, Nanchong, 637009 Sichuan, [4]College of pharmacy, Chengdu University, Chengdu, 730000 Sichuan, [5]Key-laboratory of Endangered Animal Reproduction and Conservation and Genetics, China Conservation and Research Center for the Giant Panda, Wolong, 623006 Sichuan, China

*Corresponding author, E-mail: pengxi197313@163.com

Abstract: The giant panda (*Ailuropoda melanoleuca*) is one of the most endangered species in the world. Climate change and susceptibility to disease are two of the greatest threats to this species. We performed a necropsy and histopathological examination of the organs of an old panda and investigated the pathogenesis associated with death. Necropsy and histopathological observation revealed some typical age-related lesions, such as cataract, atherosclerosis, renal insufficiency and splenic atrophy. We also confirmed hepatic lesions associated with parasitic infection. Overall, our observations revealed that the predominant cause of mortality in this panda was multiple organ dysfunction (MOD).

Key words: aged; giant panda; multiple organ dysfunction; pathology

Introduction

The giant panda (*Ailuropoda melanoleuca*) is an enigmatic carnivore, adapted to a highly specialized ecological niche (1). To date, the phylogeny, demographic history, genetic variation, population structure and adaptive evolution of the giant panda have been extensively documented (2). However, wild giant pandas remain endangered and threatened by human interference, climate change, disease, and food shortages (1, 3). Although China established its first panda sanctuary in 1987, captive breeding, especially of old animals, is a major problem for captive giant pandas (4-6). Although there are pathological studies on geriatric diseases in humans and domestic animals (7-9), pathological lesions in old giant pandas have been reported only once (5). Therefore, in this study, we investigated pathological changes associated with mortality of a deceased geriatric giant panda. The results could make an important contribution to the limited literature in this field and help to improve the welfare of giant pandas in captivity.

Received: 25 January 2021
Accepted for publication: 28 November 2022

Materials and methods

History and observed clinical signs of the panda

At this stage, we examined the life history of the giant panda, including sex and age, living conditions, treatment situation and course of the giant panda. Pathological examination revealed

that the panda was in an emaciated state and died. In addition, clinical signs, mental status, nutritional status, fur, skin, eyes, visible mucous membranes and the condition of other body surfaces, and physiological indices were observed.

Necropsy

The body of the giant panda was thoroughly visually examined. After the external visual examination, a necropsy was immediately performed, which revealed changes in various organs. The organs with visible pathological lesions were photographed with a color video camera (Nikon 3 CCD) and further examined.

Histopathology

After thorough observation at a gross visual level, we selected tissue samples for histopathology from the lung, heart, aorta, liver, kidneys, spleen, digestive tract (including esophagus, duodenum, jejunum, ileum, colon, and rectum), mesenteric lymph nodes, ovaries, subcutaneous nodular lesion, and tissue from the decubitus. Tissue samples were then fixed in 4% paraformaldehyde (PFA) solution, dehydrated in a series of alcohols (at concentrations ranging from 70% to 100%) and embedded in paraffin wax. Tissue sections (5 µm) were prepared, stained with hematoxylin and eosin (H&E) and examined under a light microscope. Histological changes were photographed using a digital camera (Olympus, Japan).

Results

History and clinical signs

The case presented for necropsy involved a female giant panda, 15 years old, rescued from a nature reserve in China in 2005. Her age was estimated based on the degree of wear of the molars and skull growth (10). As she was unable to chew bamboo, she was fed a mixture of minced bamboo leaves and concentrated feed daily. Clinical examination revealed severe cataract (Fig. 1A), which indicated that the panda was suffering from anaemia and severe cardiac, hepatic and renal insufficiencies. After timely rescue and treatment, physiological values were essentially back to normal. In 2010, she went completely blind. Later, she gradually became emaciated and

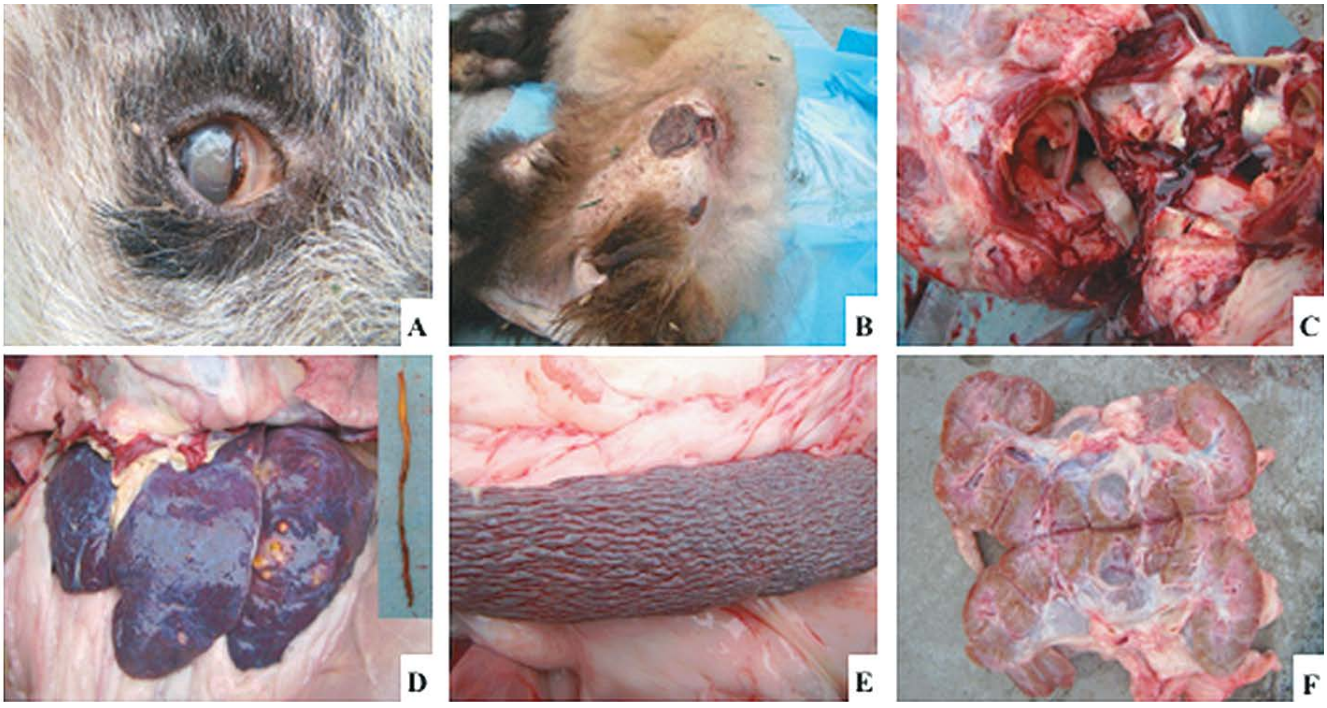

Figure 1: Gross pathological findings

A. A cataract in the right eye. B. A necrotic decubital tissue in the left gluteal region. C. Massive mucous secretion in the pharynx (arrow). D. Yellowish-white nodules on the liver surface and a nematode found in a nodule (arrow). E. The spleen shows a shrunken appearance (arrow). F. A urinoma in the left dilated kidney (arrow)

lost her fur, resulting in bald skin. In September 2013, decubital ulcers (Fig. 1B) appeared on the left buttock as a result of prolonged sleeping, which were difficult to treat. In late 2013, she fell into a deep coma and eventually died despite emergency rescue measures.

Necropsy findings

At necropsy, a large amount of viscous secretion was noted in the pharynx (Fig. 1C). The heart was enlarged and filled with blood clots. In addition, several pieces of a semitransparent jelly-like substance were seen adhering firmly to the aortic wall, showing signs of atherosclerosis. Multiple yellowish-white nodules of various sizes were observed on the surface of the liver, which contained caseous and purulent exudate and nematodes (Fig. 1D). The capsule of the spleen was contracted giving it a shrunken appearance (Fig. 1E). Both kidneys were swollen, and there were many yellowish-white mottled lesions on the surfaces. The left kidney had an enlarged pelvis filled with urine. (Fig. 1F). A single solid nodule (14×10×8 mm) was also found under the skin of the left abdomen.

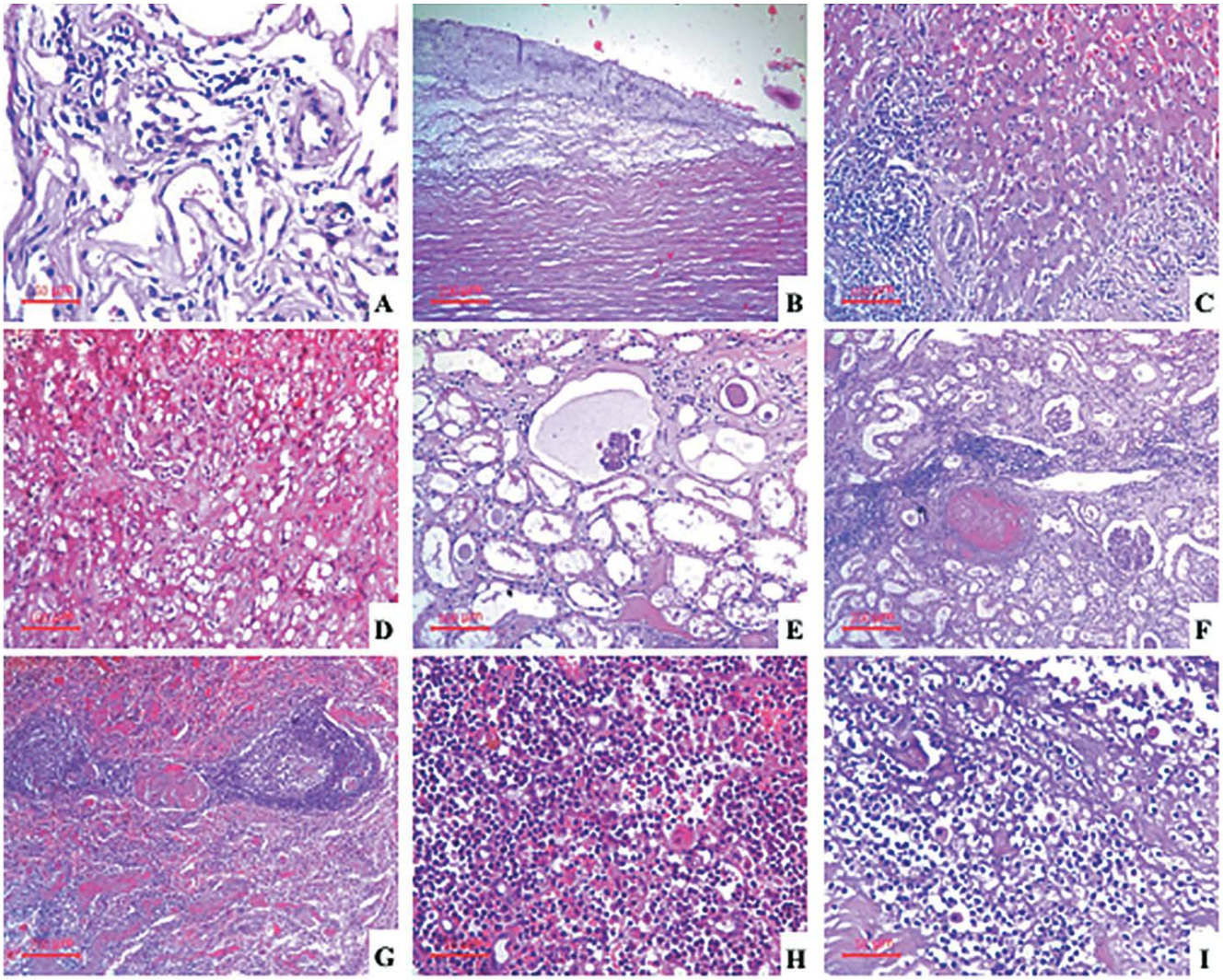

Figure 2: Histopathological changes, tissue sections stained with H&E

A. Lung. Lymphocyte infiltration and thickening of alveolar walls. B. Aorta. Atheromatous plaque. C. Liver. A proliferative nodule (square) and inflammatory cell infiltration (circle). D. Liver. Fatty degeneration (black arrow) and necrosis of hepato-cytes (blue arrow). E. Kidney. Glomerular atrophy (black arrow) and proteinaceous casts in the tubule lumina (blue arrow). F. Kidney. Hyperplasia of connective tissue (black arrow) and infiltration of inflammatory cells (blue arrow). G. Spleen. Age-related atrophy of the spleen (black arrow). H. Mesenteric lymph node. Lymphocytes (black arrow), macrophages (blue arrow), and erythrocytes (green arrow) in a lymphatic sinus. I. Decubital tissue. Numerous inflammatory cells infiltrating the necrotic muscle tissue of the decubital ulcer

Histopathological Findings

Histopathological examination of the lungs revealed slight thickening of the alveolar walls. This could be due to congestion and infiltration of inflammatory cells. Small scattered foci of inflammation were also observed, consisting mainly of lymphocytes and plasma cells, or macrophages phagocytosing black granules (Fig. 2A). In the aorta, an atheromatous plaque was noted that contained lipid-laden macrophages and proliferated connective tissue (Fig. 2B). In the liver, nodular cirrhosis with pseudohepatic lobules, fatty degeneration, and necrosis of hepatocytes was observed. Connective tissue hyperplasia, inflammatory cell infiltration, and a small focal abscess were also found in the examined tissue section of the liver (Fig. 2C and 2D). In the kidney, chronic sclerosing glomerulonephritis was diagnosed, characterized by glomerular atrophy, necrosis of the tubular epithelium, formation of proteinaceous casts, connective tissue hyperplasia, and infiltration of inflammatory cells (lymphocytes and neutrophils) (Figs. 2E and 2F). Hyperemia, abundant hemosiderin, and macrophages phagocytosing hemosiderin/erythrocytes were observed in the red pulp of the spleen (Fig. 2G). The splenic trabeculae were relatively enlarged due to age-related atrophy. Mild acute serous lymphadenitis was observed in the mesenteric lymph nodes, characterized by accumulation of lymph, fibrin, and inflammatory cells in the slightly enlarged sinuses of the lymph nodes (Fig. 2H). Only mild edema and mild exfoliation of the mucosal epithelium were noted in the digestive tract (images not shown). The single subcutaneous nodule was a benign fibroma composed of fibrocytes and desmocytes. The muscle tissue at the site of the pressure ulcer showed coagulation necrosis and inflammatory cell infiltration composed predominantly of neutrophils and macrophages (Fig. 2I).

Discussion

According to medical records, this female giant panda was about 23 years old when she died in 2013 after 8 years in captivity (11). At necropsy, massive pharyngeal mucous secretion was noted, possibly leading to the panda's asphyxiation and death. Previously, it was reported that difficulty in coughing up sputum in old pandas was due to decreased intrathoracic negative pressure, weakening of respiratory muscles and elastic retraction of the lungs (7). Lung function is known to deteriorate with age (12), and pulmonary alveolar epithelium permeability has been found to be higher in the elderly than in adults (13). It has been reported that age may play an important role in certain diseases, such as acute respiratory distress syndrome and chronic obstructive pulmonary disease (12), which is consistent with our findings in this report. In addition, some studies suggest that the lung plays an important role in the development of multiple organ dysfunction (MOD) (14, 15). MOD is more commonly reported after trauma and is associated with high mortality (16, 17). It has also been reported that the elderly are more susceptible and at higher risk of MODS (14). MOD is defined as a group of various chronic diseases, including chronic obstructive pulmonary disease and idiopathic pulmonary fibrosis (7), decreased glomeruli and tubulointerstitial fibrosis in the kidney (8), immune dysfunction and degeneration of the spleen(18), chronic heart disease (19), presbycusis (20), cataracts, and cognitive impairment (3). In our case of old giant panda, several chronic pathological changes such as cataracts, lung and kidney lesions, adipose tissue atrophy, atheromatous plaques in the aorta, and splenic atrophy were observed and reported, which developed along with parasitic infection of the liver and consequent emaciation. Histopathologically, the main findings that could be age-related were atheromatous plaques, reduction of renal glomeruli, age-related atrophy of the spleen, thickening of alveolar septa in the lungs, and connective tissue hyperplasia in the liver and kidney. These lesions were consistent with the pathological manifestations of ageing described in humans and other mammals, including giant pandas (5, 7, 8). A typical age-related change, "cataract", was due to the gradual loss of elasticity of the lens (21, 22). In addition, oxidised low-density lipoprotein (ox-LDL) has been reported to lead to endothelial dysfunction, which is considered to be an initial step in the formation of atheroma (23, 24). Ox-LDL has been shown to play an important role in the formation of lipid-laden macrophages, the primary cellular component of atherosclerotic lipid lesions (25). This may be the reason why we found the atheromatous aortic plaque in this case. We believe that the decrease in renal glomeruli in this

giant panda case is related to tubular necrosis and fibrosis, similar to some previous reports (26, 27). Age-related changes are well-known factors that influence the susceptibility to disease of almost all vital organs. The elderly individuals often show a markedly exaggerated host immune response to inflammatory stimuli (14). In the present study, the pathological lesions associated with inflammation, particularly the infiltration of inflammatory cells in the lung, kidney, liver, and lymph nodes, were possibly due to the spread of inflammation from bedsores or parasitic hepatitis to these organs. In general, systemic inflammatory response syndrome (SIRS) has been shown to have an adaptive survival function for the host, but in critically ill patients, uncontrolled production of inflammatory mediators can lead to MODS (28). The results of this study were consistent with the "2-hit" hypothesis in the development of MODS, which states that an initial insult primes the host such that a subsequent impairment, such as infection or surgery, greatly enhances the host response (18). We believe that in our case a combination of age-related pathological lesions and chronic parasitic infection led to MOD, and that MOD was the main cause of death in this old giant panda. The parasitic hepatitis could be the initial impairment, and the decubitus ulcer could be the subsequent impairment leading to increased damage, as the aging can increase susceptibility to organ dysfunction and systemic inflammation, as shown by previous reports (29, 30). The macroscopic and microscopic lesions in the liver were consistent with chronic verminous hepatitis, and it could be hypothesised that this giant panda already suffered from a parasitic infection such as the nematode *Baylisascaris schroederi* in the wild (31). In an anatomical study of 33 wild giant pandas, a 100% lumbricoid infection rate indicated the prevalence of parasitic infections in wild animals (32). A study examining causes of death in wild giant pandas from 1971 to 2005 found that the greatest threat to wild giant pandas is migration of visceral larvae (33). Consistent with the anatomical location of the nematode, the lesions found in the liver and the life cycle of the parasite (34), the parasite may have migrated from the bile duct to the liver. Currently, research in China mainly focuses on parasite species and associated morbidity in wildlife. However, in the future, more attention should also be paid to the transmission and control strategies of parasitic wildlife diseases to increase the overall life expectancy of wildlife. In addition, many infectious diseases of humans have hosts or vectors in animals, which places greater demands on research and control of animal diseases (35).

In conclusion, we believe that MOD was the main reason for the death of this old female giant panda. A series of age-related pathological lesions, supported by pre-existing pathological conditions such as liver dysfunction due to parasite infestation, eventually led to poor physical condition, emaciation, respiratory failure and death.

Acknowledgments

Authors wish to express gratitude to China Conservation and Research Center for the Giant Panda for their cooperation and assistance in conducting the study.

Supported by the program for the Education Department of Sichuan Province (project no. 17ZB0425), the Meritocracy Research Funds of China West Normal University (project no. 17YC349) and the Fundamental Research Funds of China West Normal University (project no. 20A003).

The datasets supporting the results of this document are contained within the article. Any additional data may be requested to the corresponding author.

The datasets supporting the results of this document are contained within the article. Any additional data may be requested to the corresponding author.

The authors declare no conflict of interest.

Conceptualization and supervision: W.B.Y. and P.X., Methodology, investigation, data curation, W.B.Y., W.J., C.T., W.C.D., L.D.S., D.L.H, writing-original draft preparation: W.B.Y. and W.J., writing–review and editing: P.X. All authors have read and agreed to the published version of the manuscript.

References

1. Lu Z, Warren EJ, Marilyn MR, et al. Patterns of genetic diversity in remaining giant panda populations. Conserv Biol 2001; 15(6): 1596–607.

2. Wei FW, Yibo H, Lifeng Z, Michael WB, Zan XJ, Lei Z. Black and white and read all over: the

past, present and future of giant panda genetics. Mol Ecol 2012; 21(23): 5660–74.

3. Steinmeyer C, Pennings PS, Foitzik S. Multicolonial population structure and nestmate recognition in an extremely dense population of the European ant *Lasius flavus*. Insect Soc 2012; 59(4): 499–510.

4. Burrell C, Hemin Z, Desheng L, Chengdong W, Caiwu L, Aitken-Palmer C. Hematology, serum biochemistry, and urinalysis value in the giant panda (*Ailuropoda melanoleuca*). J Zoo Wildlife Med 2017; 48(4): 1072–6.

5. Guo DZ, Shiqi Z, Jiakui L, Xueying H, Shijin Y. Pathology observation on multiple organ faliure of aging giant panda. Chinese J Anim Vet Sci 2002; 33(3): 295–8.

6. Liu DZ, Guiquan Z, Rongping W, Hemin Z, Jiming F, Ruyong S. Effects of sex and age on the behavior of captive giant pandas (*Ailuropoda melanoleuca*). Acta Zool Sin 2012; 48(5): 585–90.

7. Britto RR, Zampa CC, de Oliveira TA, Prado LF, Parreira VF. Effects of the aging process on respiratory function. Gerontology 2009; 55(5): 505–10.

8. Weinstein JR, Sharon A. The aging kidney: physiological changes. Adv Chronic Kidney Dis 2010; 17(4): 302–7.

9. Föllmi J, Steiger A, Walzer C, et al. A scoring system to evaluate physical condition and quality of life in geriatric zoo mammals. Anim Welfare 2007; 16(3): 309–18.

10. Wei FW, Jinchu H, Guangzan X, Mingdao J, Qitao D, Zhaomin Z. The age of determination for giant panda. Acta Theriol Sin 1989; 8(3): 161–5.

11. Zhou X, Yan H, Jingyan H, Shiqiang Z, Dian L. Behavioral development of gaint panda and influencing factors in husbandry management. J Heilongjiang Univ Sci Technol 2013; 34(2): 106–10.

12. Sevransky JE, Haponik EF. Respiratory failure in elderly patients. Clin Geriatr Med 2003; 19(1): 205–24.

13. Yang MF, He ZX, Wang SW. Evaluation of pulmonary epithelial permeability with 99Tc-m-DTPA radioaerosol. Chin J Nucl Med 2002; 22(4): 250–2.

14. Wang XP, Zhu QL, Xue Q, et al. Role of the lung in the progression of multiple organ dysfunction syndrome in ageing rat model. Chin Med J 2012; 125(015): 2708–13.

15. Wang SW, Han YL, Qian XS, et al. Clinical features of multiple organ failure in the elderly: a report of 1605 cases. Chin J Mult Organ Dis Elderly 2002; 1(1): 7–10.

16. Durham RM, Moran JJ, Mazuski JE, Shapiro MJ, Baue AE, Flint LM. Multiple organ failure in trauma patients. J Trauma Acute Care 2003; 55(4): 608–16.

17. Goris RJA. Pathophysiology of multi-organ failure: an overview. Clin Intensive Care 1991; 2(6): 5–15.

18. Zhu H, Pin Y, Yanfeng X, et al. Structual and functional changes of immune system in natural aged SD rats. Acta Laborator Anim Sci Sin 2018; 26(1): 95–100.

19. Stewart S, MacIntyre K, Capewell S, McMurray JJV. Heart failure and the aging population: an increasing burden in the 21st century? Heart 2003; 89(1): 49–53.

20. van Boxtel MV, Buntinx F, Houx P, Metsemakers J, Knottnerus A, Jolles J. The relation between morbidity and cognitive performance in a normal aging population. J Gerontol A Biol 1998; 53(2): 147–54.

21. Truscott RJW. Eye lens proteins and cataracts. In: Uversky VN, Fink AL, eds. Protein misfolding, aggregation, and conformational diseases. Boston : Springer, 2006: 435–47. (Protein Reviews, vol. 6) doi: 10.1007/978-0-387-36534-3_21

22. Olcaysu OO, Kivanc SA, Altun A, Cinici E, Altinkaynak H and Ceylan E. Causes of disability, low vision and blindness in old age. Turk J Geriatr 2014; 17(1): 44–9.

23. Cao C, Qi Y, Chen W, Zhu Y and Chen X. Effects of IKK on oxidised low-density lipoprotein-induced injury in vascular endothelial cells. Heart Lung Circ 2013; 22(5): 366–72.

24. Toth PP. Low-density lipoprotein reduction in high-risk patients: how low do you go?. Curr Atheroscler Rep 2004; 6(5): 348–52.

25. Derian CK, Lewis DF. Activation of 15-lipoxygenase by low density lipoprotein in vascular endothelial cells. Relationship to the oxidative modification of low density lipoprotein. Prostag Leukotr ESS 1992; 45(1): 49–57.

26. Zhou C, Wu J, Torres L, et al. Blockade of osteopontin inhibits glomerular fibrosis in a model of anti-glomerular basement membrane glomerulonephritis. Am J Nephrol 2010; 32(4): 324–31.

27. Kanbay M, Kasapoglu B, Perazella MA. Acute tubular necrosis and pre-renal acute kidney injury: utility of urine microscopy in their evaluation-a systematic review. Int Urol Nephrol 2010; 42(2): 425–33.

28. Nathens AB, Marshall JC. Sepsis, SIRS, and MODS: What's in a name? World J Surg 1999; 20(4): 386–91.

29. Nin N, Lorente JA, De Paula M, et al. Aging increases the susceptibility to injurious mechanical ventilation. Intensive Care Med 2008; 34(5): 923–31.

30. Eachempati SR, Hydo LJ, Shou J, Barie PS. Outcomes of acute respiratory distress syndrome (ARDS) in elderly patients. J Trauma 2007; 63(2): 344–50.

31. Zhou X, Yu H, Wang N, Xie Y, Yang GY. Molecular diagnosis of *Baylisascaris schroederi* infections in giant panda *(Ailuropoda melanoleuca*) feces using PCR. J Wildl Dis 2013; 49(4): 1052–5.

32. Feng WH, Anju Z, eds. Giant panda reproduction and disease research. Chengdu, Sichuan, China : Sichuan Science and Technology Press, 1991: 244–8.

33. Zhang JS, Peter D, Huali H, Guangyou Y, A Marm K, Shuyi Z. Parasite threat to panda conservation. EcoHealth 2007; 5(1): 6–9.

34. Blouin MS, Liu J, Berry RE. Life cycle variation and the genetic structure of nematode populations. Heredity 1999; 83(3): 253–9.

35. Kaupke A, Rzezutka A. Epidemiology of the invasion of *Cryptosporidium parvum* in farm and wild animals. Med Weter 2017; 73(7): 387–94.

PATOLOŠKE UGOTOVITVE PRI SAMICI VELIKEGA PANDE – POROČILO O PRIMERU

B. Wu, J. Wang, T. Cai, C. Wang, D. Li, L. Deng, X. Peng

Izvleček: Veliki panda (*Ailuropoda melanoleuca*) je ena najbolj ogroženih vrst na svetu. Vrsto najbolj ogrožajo podnebne spremembe in dovzetnost za bolezni. Opravili smo nekropsijo in histopatološki pregled organov starega pande ter raziskali patogenezo, povezano s smrtjo. Z nekropsijo in histopatološkim opazovanjem smo odkrili nekatere značilne starostne spremembe, kot so katarakta, ateroskleroza, ledvična insuficienca in atrofija vranice. Potrdili smo tudi jetrne spremembe, povezane s parazitsko okužbo. Naša opažanja so pokazala, da je bil prevladujoči vzrok smrti tega pande disfunkcija več organov (MOD).

Ključne besede: star; veliki panda; disfunkcija več organov; patologija

AUTHOR INDEX VOLUME 59, 2022

Abo-Kora SY, see El-Bahr SM, Al-Sultan S, Hamouda AF, Atwa SAE, Abo-Kora SY, Amin AA, Shousha S, Alhojaily S, Alnehas A, Elzogby RR 195

Aja PM, see Alum EU, Ibiam UA, Ugwuja EI, Aja PM, Igwenyi IO, Offor CE, Orji OU, Aloke C, Ezeani NN, Ugwu OPC, Egwu CO.....31

Akbalık ME, see Topaloğlu U, Ketani MA, Akbalık ME, Sağsöz H, Saruhan BG, Bayram B 99

Akyol ET, see Parlak K, Yalcin M, Akyol ET, Ok M, Arican M 185

Alakuş İ, see Deveci MZY, Yurtal Z, İşler CT, Emiroğlu SB, Alakuş İ, Altuğ ME 47

Alhojaily S, see El-Bahr SM, Al-Sultan S, Hamouda AF, Atwa SAE, Abo-Kora SY, Amin AA, Shousha S, Alhojaily S, Alnehas A, Elzogby RR.....195

Alkan S, see Karabağ K, Alkan S, Karslı T, İkten C, Şahin İ, Mendeş M 89

Alnehas A, see El-Bahr SM, Al-Sultan S, Hamouda AF, Atwa SAE, Abo-Kora SY, Amin AA, Shousha S, Alhojaily S, Alnehas A, Elzogby RR.....195

Aloke C, see Alum EU, Ibiam UA, Ugwuja EI, Aja PM, Igwenyi IO, Offor CE, Orji OU, Aloke C, Ezeani NN, Ugwu OPC, Egwu CO.....31

Al-Sultan S, see El-Bahr SM, Al-Sultan S, Hamouda AF, Atwa SAE, Abo-Kora SY, Amin AA, Shousha S, Alhojaily S, Alnehas A, Elzogby RR.....195

Altuğ ME, see Deveci MZY, Yurtal Z, İşler CT, Emiroğlu SB, Alakuş İ, Altuğ ME.....47

Alum EU, Ibiam UA, Ugwuja EI, Aja PM, Igwenyi IO, Offor CE, Orji OU, Aloke C, Ezeani NN, Ugwu OPC, Egwu CO. Antioxidant effect of Buchholzia coriacea ethanol leaf-extract and fractions on freund's adjuvant-induced arthritis in albino rats: A comparative stdy.....31

Amin AA, see El-Bahr SM, Al-Sultan S, Hamouda AF, Atwa SAE, Abo-Kora SY, Amin AA, Shousha S, Alhojaily S, Alnehas A, Elzogby RR.....195

Andrásofszky E, see Hetényi N, Andrásofszky E...137

Arican M, see Parlak K, Yalcin M, Akyol ET, Ok M, Arican M.....185

Atwa SAE, see El-Bahr SM, Al-Sultan S, Hamouda AF, Atwa SAE, Abo-Kora SY, Amin AA, Shousha S, Alhojaily S, Alnehas A, Elzogby RR.....195

Bayram B, see Topaloğlu U, Ketani MA, Akbalık ME, Sağsöz H, Saruhan BG, Bayram B.....99

Beqiraj D, see Sulçe M, Munga A, Beqiraj D, Ozuni E, Zalla P, Muça G, Koleci X.....129

Cai T, see Wu B, Wang J, Cai T, Wang C, Li D, Deng L, Peng X.....211

Deng L, see Wu B, Wang J, Cai T, Wang C, Li D, Deng L, Peng X.....211

Deveci MZY, Yurtal Z, İşler CT, Emiroğlu SB, Alakuş İ, Altuğ ME. Herniorrhaphy and surgical outcomes of diaphragmatic hernia in cats.....47

Egwu CO, see Alum EU, Ibiam UA, Ugwuja EI, Aja PM, Igwenyi IO, Offor CE, Orji OU, Aloke C, Ezeani NN, Ugwu OPC, Egwu CO.....31

Eid HM, El-Mahallawy HS, Elsheshtawy HM, Shalaby AM, Shetewy MM, Eidaroos NH. Antimicrobial resistance and virulence-associated genes of aeromonads isolated from Lake Manzala water and wild Nile tilapia: Implications to public health and the lake microbial community.....59

Eidaroos NH, see Eid HM, El-Mahallawy HS, Elsheshtawy HM, Shalaby AM, Shetewy MM, Eidaroos NH.....59

El-Bahr SM, Al-Sultan S, Hamouda AF, Atwa SAE, Abo-Kora SY, Amin AA, Shousha S, Alhojaily S, Alnehas A, Elzogby RR. Pectin improves hemato--biochemical parameter, histopathology, oxidative stress biomarkers, cytokines and expression of hepcidin gene in lead induced toxicity in rats.....195

El-Ghany WAA. Avian cryptosporidiosis: a significant parasitic disease of public health hazard.....5

El-Mahallawy HS, see Eid HM, El-Mahallawy HS, Elsheshtawy HM, Shalaby AM, Shetewy MM, Eidaroos NH.....59

Elsheshtawy HM, see Eid HM, El-Mahallawy HS, Elsheshtawy HM, Shalaby AM, Shetewy MM, Eidaroos NH.....59

Elzogby RR, see El-Bahr SM, Al-Sultan S, Hamouda AF, Atwa SAE, Abo-Kora SY, Amin AA, Shousha S, Alhojaily S, Alnehas A, Elzogby RR.....195

Emiroğlu SB, see Deveci MZY, Yurtal Z, İşler CT, Emiroğlu SB, Alakuş İ, Altuğ ME.....47

Ezeani NN, see Alum EU, Ibiam UA, Ugwuja EI, Aja PM, Igwenyi IO, Offor CE, Orji OU, Aloke C, Ezeani NN, Ugwu OPC, Egwu CO.....31

Hamouda AF, see El-Bahr SM, Al-Sultan S, Hamouda AF, Atwa SAE, Abo-Kora SY, Amin AA, Shousha S, Alhojaily S, Alnehas A, Elzogby RR.....195

Hetényi N, Andrásofszky E. Evaluation of commercial tortoise and turtle feeds.....137

Ibiam UA, see Alum EU, Ibiam UA, Ugwuja EI, Aja PM, Igwenyi IO, Offor CE, Orji OU, Aloke C, Ezeani NN, Ugwu OPC, Egwu CO.....31

Igwenyi IO, see Alum EU, Ibiam UA, Ugwuja EI, Aja PM, Igwenyi IO, Offor CE, Orji OU, Aloke C, Ezeani NN, Ugwu OPC, Egwu CO.....31

Igwenyi IO, see Alum EU, Ibiam UA, Ugwuja EI, Aja PM, Igwenyi, IO, Offor CE, Orji OU, Aloke C, Ezeani NN, Ugwu OPC, Egwu CO.....31

İkten C, see Karabağ K, Alkan S, Karslı T, İkten C, Şahin İ, Mendeş M.....89

İşler CT, see Deveci MZY, Yurtal Z, İşler CT, Emiroğlu SB, Alakuş İ, Altuğ ME.....47

Karabağ K, Alkan S, Karslı T, İkten C, Şahin İ, Mendeş M. Effects of selection in terms of meat yield traits on leptin receptor gene in Japanese quail lines.....89

Karslı T, see Karabağ K, Alkan S, Karslı T, İkten C, Şahin İ, Mendeş M.....89

Ketani MA, see Topaloğlu U, Ketani MA, Akbalık ME, Sağsöz H, Saruhan BG, Bayram B.....99

Koleci X, see Sulçe M, Munga A, Beqiraj D, Ozuni E, Zalla P, Muça G, Koleci X.....129

Li D, see Wu B, Wang J, Cai T, Wang C, Li D, Deng L, Peng X.....211

Li Y, see Munibullah M, Li Y, Munib K, Zhang Z...75

Mendeş M, see Karabağ K, Alkan S, Karslı T, İkten C, Şahin İ, Mendeş M.....89

Milevoj N, Tozon N, Tomsič K. Use of cannabidiol products by pet owners in Slovenia: a survey-based study.....149

Muça G, see Sulçe M, Munga A, Beqiraj D, Ozuni E, Zalla P, Muça G, Koleci X.....129

Munga A, see Sulçe M, Munga A, Beqiraj D, Ozuni E, Zalla P, Muça G, Koleci X.....129

Munib K, see Munibullah M, Li Y, Munib K, Zhang Z.....75

Munibullah M, Li Y, Munib K, Zhang Z. Regional epidemiology and associated risk factors of peste des petits ruminants in Asia – Areview.....75

Naseri A, see Parlak K, Yalcin M, Akyol ET, Ok M, Arican M.....185

Offor CE, see Alum EU, Ibiam UA, Ugwuja EI, Aja PM, Igwenyi IO, Offor CE, Orji OU, Aloke C, Ezeani NN, Ugwu OPC, Egwu CO.....31

Ok M, see Parlak K, Yalcin M, Akyol ET, Ok M, Arican M.....185

Orji OU, see Alum EU, Ibiam UA, Ugwuja EI, Aja PM, Igwenyi IO, Offor CE, Orji OU, Aloke C, Ezeani NN, Ugwu OPC, Egwu CO.....31

Ozuni E, see Sulçe M, Munga A, Beqiraj D, Ozuni E, Zalla P, Muça G, Koleci X.....129

Parlak K, Naseri A, Yalcin M, Akyol ET, Ok M, Arican M. Evaluation of trauma scoring and endothelial glycocalyx injury in cats with head trauma.....185

Peng X, see Wu B, Wang J, Cai T, Wang C, Li D, Deng L, Peng X.....211

Rajčević U, Smole A. Preclinical mouse models in adoptive cell therapies of cancer.....173

Sağsöz H, see Topaloğlu U, Ketani MA, Akbalık ME, Sağsöz H, Saruhan BG, Bayram B.....99

Şahin İ, see Karabağ K, Alkan S, Karslı T, İkten C, Şahin İ, Mendeş M.....89

Saruhan BG, see Topaloğlu U, Ketani MA, Akbalık ME, Sağsöz H, Saruhan BG, Bayram B.....99

Shalaby AM, see Eid HM, El-Mahallawy HS, Elsheshtawy HM, Shalaby AM, Shetewy MM, Eidaroos NH.....59

Shetewy MM, see Eid HM, El-Mahallawy HS, Elsheshtawy HM, Shalaby AM, Shetewy MM, Eidaroos NH.....59

Shousha S, see El-Bahr SM, Al-Sultan S, Hamouda AF, Atwa SAE, Abo-Kora SY, Amin AA, Shousha S, Alhojaily S, Alnehas A, Elzogby RR.....195

Smodiš Škerl MI, Tlak Gajger I. Performance and Nosema spp. spore level in young honeybee (Apis mellifera carnica, Pollmann 1879) colonies supplemented with candies.....159

Smole A, see Rajčević U,. Preclinical mouse models in adoptive cell therapies of cancer.....173

Sulçe M, Munga A, Beqiraj D, Ozuni E, Zalla P, Muça G, Koleci X. Applicability of flow cytometry in identifying and staging lymphoma, leukemia and mast cell tumors in dogs: an overview.....129

Tlak Gajger I, see Smodiš Škerl MI, Tlak GajgerI.....159

Tomsič K, see Milevoj N, Tozon N, Tomsič K.....149

Topaloğlu U, Ketani MA, Akbalık ME, Sağsöz H, Saruhan BG, Bayram B. Immunolocalization of HOXA11 and HLX prot ins in cow placenta during pregnancy.....99

Tozon N, see Milevoj N, Tozon N, Tomsič K.....149

Ugwu OPC, see Alum EU, Ibiam UA, Ugwuja EI, Aja PM, Igwenyi IO, Offor CE, Orji OU, Aloke C, EzeaniNN, UgwuOPC, EgwuCO.....31

Ugwuja EI, see Alum EU, Ibiam UA, Ugwuja EI, Aja PM, Igwenyi, IO, Offor CE, Orji OU, Aloke C, EzeaniNN, UgwuOPC, EgwuCO.....31

Uršič M. Morphometrical features of the cave bear and brown bear head skeleton: A comparative study.....113

Wang C, see Wu B, Wang J, Cai T, Wang C, Li D, Deng L, Peng X.....211

Wang J, see Wu B, Wang J, Cai T, Wang C, Li D, Deng L, Peng X.....211

Wu B, Wang J, Cai T, Wang C, Li D, Deng L, Peng X. Pathological findings in an old female giant panda – a case report.....211

Yalcin M, see Parlak K, Yalcin M, Akyol ET, Ok M, Arican M.....185

Yurtal Z, see Deveci MZY, Yurtal Z, İşler CT, EmiroğluSB, Alakuşİ, AltuğME.....47

Zalla P, see Sulçe M, Munga A, Beqiraj D, Ozuni E, Zalla P, Muça G, Koleci X.....129

Zhang Z, see Munibullah M, Li Y, Munib K, Zhang Z.....75

SLOVENIAN VETERINARY RESEARCH
SLOVENSKI VETERINARSKI ZBORNIK

Slov Vet Res 2022; 59 (4)

Review Article

Rajčević U, Smole A. Preclinical mouse models in adoptive cell therapies of cancer 173

Original Research Articles

Parlak K, Naseri A, Yalcin M, Akyol E T, Ok M, Arican M. Evaluation of trauma scoring and endothelial glycocalyx injury in cats with head trauma 185

El-Bahr SM, Al-Sultan S, Hamouda AF, Atwa SAE, Abo-Kora SY, Amin AA, Shousha S, Alhojaily S, Alnehas A, Elzogby RR. Pectin improves hemato-biochemical parameter, histopathology, oxidative stress biomarkers, cytokines and expression of hepcidin gene in lead induced toxicity in rats 195

Case Report

Wu B, Wang J, Cai T, Wang C, Li D, Deng L, Peng X. Pathological findings in an old female giant panda – a case report 211

Author Index Volume 59, 2022 219